Title

Perinatal exposure to organohalogen pollutants decreases vasopressin content and its mRNA expression in magnocellular neuroendocrine cells activated by osmotic stress in adult rats.

Authors

Mucio-Ramírez, Samuel
Sánchez-Islas, Eduardo
Sánchez-Jaramillo, Edith
et al.

Publication Date

2017-08-01

DOI

10.1016/j.taap.2017.05.039

Peer reviewed

Toxicology and Applied Pharmacology 329 (2017) 173–189

Contents lists available at ScienceDirect

Toxicology and Applied Pharmacology

journal homepage: www.elsevier.com/locate/taap

Perinatal exposure to organohalogen pollutants decreases vasopressin content and its mRNA expression in magnocellular neuroendocrine cells activated by osmotic stress in adult rats

Samuel Mucio-Ramírez [a], Eduardo Sánchez-Islas [a], Edith Sánchez-Jaramillo [b], Margarita Currás-Collazo [c], Victor R. Juárez-González [d], Mhar Y. Álvarez-González [a], L.E. Orser [c], Borin Hou [c], Francisco Pellicer [e], Prasada Rao S. Kodavanti [f], Martha León-Olea [a,*]

[a] Departamento de Neuromorfología Funcional, Dirección de Investigaciones en Neurociencias, Instituto Nacional de Psiquiatría Ramón de la Fuente Muñiz, Calz. México Xochimilco No. 101, Col. San Lorenzo Huipulco, México D.F. C.P. 14370, México
[b] Laboratorio de Neuroendocrinología Molecular, Dirección de Investigaciones en Neurociencias, Instituto Nacional de Psiquiatría Ramón de la Fuente Muñiz, Calz. México Xochimilco No. 101, Col. San Lorenzo Huipulco. México D.F. C.P. 14370, México
[c] Department of Cell Biology and Neuroscience, University of California, Riverside, CA 92521, USA
[d] Medicina Molecular y Bioprocesos, Instituto de Biotecnología, UNAM, Av. Universidad #2001, Col. Chamilpa, C.P. 62210 Cuernavaca, Morelos, México
[e] Laboratorio de Fisiología Integrativa, Dirección de Investigaciones en Neurociencias, Instituto Nacional de Psiquiatría Ramón de la Fuente Muñiz. Calz. México Xochimilco No. 101, Col. San Lorenzo Huipulco, México D.F. C.P. 14370, México
[f] Neurotoxicology Branch, Toxicity Assessment Division, NHEERL/ORD, US Environmental Protection Agency, Research Triangle Park, NC 27711, USA

ARTICLE INFO

Article history:
Received 2 December 2016
Revised 29 May 2017
Accepted 31 May 2017
Available online 1 June 2017

Keywords:
Vasopressin
Neuroendocrine disruption
PCBs
PBDEs
Salt loading
cFOS

ABSTRACT

Polychlorinated biphenyls (PCBs) and polybrominated diphenyl ethers (PBDEs) are environmental pollutants that produce neurotoxicity and neuroendocrine disruption. They affect the vasopressinergic system but their disruptive mechanisms are not well understood. Our group reported that rats perinatally exposed to Aroclor-1254 (A1254) and DE-71 (commercial mixtures of PCBs and PBDEs) decrease somatodendritic vasopressin (AVP) release while increasing plasma AVP responses to osmotic activation, potentially emptying AVP reserves required for body-water balance. The aim of this research was to evaluate the effects of perinatal exposure to A1254 or DE-71 (30 mg kg/day) on AVP transcription and protein content in the paraventricular and supraoptic hypothalamic nuclei, of male and female rats, by in situ hybridization and immunohistochemistry. cFOS mRNA expression was evaluated in order to determine neuroendocrine cells activation due to osmotic stimulation. Animal groups were: vehicle (control); exposed to either A1254 or DE-71; both, control and exposed, subjected to osmotic challenge. The results confirmed a physiological increase in AVP-immunoreactivity (AVP-IR) and gene expression in response to osmotic challenge as reported elsewhere. In contrast, the exposed groups did not show this response to osmotic activation, they showed significant reduction in AVP-IR neurons, and AVP mRNA expression as compared to the hyperosmotic controls. cFOS mRNA expression increased in A1254 dehydrated groups, suggesting that the AVP-IR decrease was not due to a lack of the response to the osmotic activation. Therefore, A1254 may interfere with the activation of AVP mRNA transcript levels and protein, causing a central dysfunction of vasopressinergic system.

1. Introduction

The maintenance of water homeostasis is vital for living beings. The neuropeptides secreted by the hypothalamic-neurohypophysial system, vasopressin (AVP) and oxytocin (OXT), play key roles in homeostasis and fine-tuning of osmotic regulation (Bourque, 2008; Schrier and Martin, 1998; Weitzman and Kleeman, 1979). These neuropeptides exert a wide range of actions and control not only upon water and sodium excretion by the kidneys, they also influence cardiovascular

* Corresponding author at: Departamento de Neuromorfología Funcional, Dirección de Investigaciones en Neurociencias, Instituto Nacional de Psiquiatría Ramón de la Fuente Muñiz, Calz. México Xochimilco No. 101, Col. San Lorenzo Huipulco, México D.F. C.P. 14370, México.
E-mail addresses: mucios@imp.edu.mx (S. Mucio-Ramírez), edaxy@imp.edu.mx (E. Sánchez-Islas), esanchez@imp.edu.mx (E. Sánchez-Jaramillo), margarita.curras@ucr.edu (M. Currás-Collazo), rivelino@ibt.unam.mx (V.R. Juárez-González), mhar123@hotmail.com (M.Y. Álvarez-González), pellicer@imp.edu.mx (F. Pellicer), Kodavanti.Prasada@epa.gov (P.R.S. Kodavanti), marthalo@imp.edu.mx (M. León-Olea).

http://dx.doi.org/10.1016/j.taap.2017.05.039
0041-008X/

responses, learning and memory, thermoregulation, social, sexual, reproductive behavior and stress-related responses, among others (Cunningham and Sawchenko, 1991; Pittman and Bagdan, 1992; Riphagen and Pittman, 1986; Neumann and Landgraf, 2012; Witt, 1995). Osmotic and volume stimuli, such as dehydration and hemorrhage, activate magnocellular neuroendocrine cells (MNCs) in the paraventricular (PVN) and supraoptic nuclei (SON) of the hypothalamus. In response to this activation, MNCs produce both AVP and OXT that are released into the systemic circulation from axon terminals located in the neurohypophysis and within the PVN and the SON from soma and dendrites (somatodendritic release) (Hatton et al., 1978; Ludwig and Leng, 1998; Ludwig et al., 1994). Somatodendritic AVP exerts autoinhibitory control over plasma AVP hormonal output. Therefore, the central and peripheral AVP are essential to maintain osmoregulation (Ludwig and Leng, 1998; Riphagen and Pittman, 1986; Wotjak et al., 1994).

It has been well established that a wide variety of environmental pollutants have specific effects on the neuroendocrine systems of mammals, therefore, the concept of neuroendocrine disruptors was developed (Leon-Olea et al., 2014; Currás-Collazo, 2011; Waye and Trudeau, 2011). Industrial organohalogens such as polychlorinated biphenyls (PCBs) and polybrominated diphenyl ethers (PBDEs), widely used as flame retardants, are neurotoxic agents and neuroendocrine disruptors that pollute outdoor and indoor environments (de Wit et al., 2012; Birnbaum and Staskal, 2004). They are lipophilic and bioaccumulate in wildlife and humans (de Wit, 2002; Kodavanti et al., 1998; Tilson et al., 1998). After two accidental contamination incidents that lead to death and several adverse health effects in humans, PCBs were banned from production in 1977 but still linger in human tissues and the environment (Lang, 1992; Mariussen and Fonnum, 2006; Safe, 1993; Wu et al., 2011). PBDEs are similar in structure to PCBs but the bromide radical substitutes for chloride (Covaci et al., 2011; Wiseman et al., 2011). The current commercial formulation of PBDEs is decaBDE (10 bromines). PentaBDE and octaBDE (5, 8 bromines respectively) were voluntarily withdrawn from the market in 2004 (U.S. Environmental Protection Agency, USEPA, 2010). These pollutants, as the PCBs, are added to household appliances, furniture, textiles, plastics, electronic devices and packaging materials, thus it is a major source of the indoor pollution that affects humans, especially infants and toddlers (Birnbaum and Staskal, 2004; de Wit et al., 2012). PCBs and PBDEs have been detected in human blood, adipose tissue, and they cross through the placental barrier and in to breast milk (Jacobson et al., 1984; Kodavanti et al., 1998; Takagi et al., 1986). They disrupt brain development, learning and memory, and the reproductive and endocrine systems via alterations in thyroid, growth, and reproductive hormones (Chung et al., 2001; Hamers et al., 2006; Kodavanti et al., 2010; Kodavanti and Curras-Collazo, 2010; Ness et al., 1993; Steinberg et al., 2007; Viberg et al., 2006). The effects of these organohalogens depend on factors such as dosage, sex, susceptibility of each organism, type of congener, duration of exposure, physiological activation, and life stage at which the organism is exposed (Faroon et al., 2001; McKinney and Waller, 1994; Viberg et al., 2006). PCBs and PBDEs produce neurotoxicity by disrupting protein kinase C (PKC) and perturbing intracellular calcium homeostasis, nitric oxide signaling, neurotransmitter release, synaptic plasticity, gene expression, oxidative stress, and energy metabolism in the brain (Coburn et al., 2008, 2015; Kodavanti et al., 2011; Royland and Kodavanti, 2008; Tilson et al., 1998; Westerink, 2014; Wong et al., 1997).

Organohalogens also disrupt the vasopressinergic system (Coburn et al., 2007; Coburn et al., 2005; Kodavanti and Curras-Collazo, 2010). We have previously reported that exposure to Aroclor 1254 (A1254) and DE-71, commercial mixtures of PCBs and PBDEs respectively, increases plasma vasopressin release, and decrease somatodendritic AVP release during hyperosmotic stimulation in adult rats, suggesting that PCBs and PBDEs could disrupt signaling mechanisms required for AVP release in response to an osmotic stimulus (Coburn et al., 2007; Coburn et al., 2005). Moreover, perinatal exposure to PBDEs alters AVP-related functions, producing exaggerated cardiovascular reactivity and compromised osmoregulatory capacity in late-adulthood rats (Shah et al., 2011). The mechanisms by which PCBs and PBDEs disrupt the vasopressinergic system remain unknown. Based on our previous report showing elevated plasma and reduced somatodendritic vasopressin in response to these pollutants, we hypothesize that these organohalogens may disrupt the AVP transcription and/or protein content in the PVN and SON cells populations in rats with prolonged or acute hyperosmotic challenge. Therefore, the aim of this research was to elucidate the effects of perinatal exposure to either A1254 or DE-71 (30 mg kg/day) on AVP gene and protein responses to osmotic stimulation in the rat PVN and SON hypothalamic nuclei.

2. Materials and methods

2.1. Animals

The experimental animals were maintained under controlled laboratory conditions with a light-dark (12:12 h) cycle and ad libitum access to water and a regular diet (commercial pellets Lab Chow 5001 Purina USA). A group of time-pregnant Wistar rats on gestational day (GD) two (based on a GD 0, as the day of insemination, indicated by copulatory plug) was obtained from the animal care facility of INPRFM, México (cohort I and cohort III). In parallel, a group of timed-pregnant Sprague-Dawley (SD) rats (cohort II), a subspecies of Wistar with similar physiology and behavior (Andersen and Tufik, 2016), was reared at the animal care facility of the University of California, Riverside (UCR). The experiments were performed in accordance with NIH guidelines for care and use of laboratory animals and with the approval of the Projects and Ethics Committee of the INPRFM and the IACUC of the UCR.

2.2. Chemicals

Commercial PCB mixture, Aroclor 1254 (purity > 99%; Lot: 124-191-B), was obtained from Accustandard, New Haven, CT. The constituent PCB congeners (pg/ng) based on ortho-substitutions in this PCB mixture were: non-ortho 0.02%; mono-ortho 24.1%; di-ortho 53.8%; tri-ortho 21.2%; tetra-ortho 0.85% (Kodavanti et al., 2001). Commercial PBDE mixture, DE-71 (technical pentabromodiphenyl oxide; CAS no. 32534-81-9; Lot 2550OA30A) was obtained from Great Lakes Chemical Corporation, West Lafayette, IN. The composition of individual congeners in DE-71 was: PBDE-47 (36%); PBDE-99 (42%); PBDE-100 (10%); PBDE-153 (3%); PBDE-154 (4%); and PBDE-85 (2%). The remaining 3% consists of several identified tri-heptaBDEs and some unidentified PBDEs (Dunnick et al., 2012).

2.3. Perinatal exposure to A1254 and DE-71

Perinatal exposure was accomplished by feeding pregnant dams (n = 25, Wistar and n = 8, SD) with snacks (popcorn or Cheetos) infused with A1254 (30 mg/kg/day) dissolved in corn oil vehicle or infused with vehicle only (controls), for 10 days during gestation (GD 10-19) (cohort I, II). Although A1254 was administered prenatally, the offspring was still exposed via breast milk. Several studies have shown that PCBs have a longer half-life (Tanabe et al., 1981) and slowly decrease in breast milk throughout lactation (LaKind et al., 2009; Takagi et al., 1986). Due to this, A1254 exposure was considered as perinatal exposure. Cohort III: Wistar pregnant dams (n = 10), received snacks dosed with the commercial penta-PBDE mixture DE-71 (30 mg/kg/d) dissolved in corn oil vehicle or with vehicle only (control), from GD 6 to postnatal day (PND) 21. The volume of each dosing mixture in corn oil was adjusted based on changes in the dam's weight. The pups were weaned and separated by sex at PND-22 and were allowed to mature until 3–5 months old.

The dosing and experimental paradigm used in this study match the experimental conditions in our previous reports (Coburn et al., 2015; Kodavanti et al., 2010; Shah et al., 2011). Kodavanti et al. (1998) where we showed that adult rats dosed orally with A1254 (30 mg/kg/day for 20 days), have brain tissue concentrations of 8.2–15.1 ppm or 20–50 μM. Such tissue concentrations have been shown to disrupt neuronal signaling without producing overt cell death (Kodavanti and Tilson, 2000). For reference, brain PCB levels of up to 29.5 ppm (w/w) and until 80 ppm (fat weight basis) have been found in wildlife exhibiting overt neurological symptoms (Gabrielsen et al., 1995; Skaare et al., 2000; Kodavanti, 2005). For PBDEs in a regimen of 50 ppm in food pellets from gestational day 8 to postnatal day 14, brain tissue concentration was 1.2 μg/g weight tissue (Rickert et al., 1978). We used this high dose and the same lot numbers of A1254 or DE-71 that were proven to produce neurotoxicity in previous studies (Kodavanti et al., 2010; 2001; Kodavanti and Ward, 2005). Delivery of toxicants via dietary snacks has consistently proven to be an effective method of oral exposure in our lab and others using different snacks or mixed in pellets (Coburn et al., 2015; Coburn et al., 2005; Kodavanti et al., 2010; Rickert et al., 1978). A1254 at 30 mg/kg/day of exposure could reduce litter size (Brezner et al., 1984). Therefore, at PND 4 the offspring number was adjusted to eight pups per dam. The pup ratio was 60% females and 40% males (4–5 females/l).

At 3–5 months of age (250–450 g), the pups of the litters were randomly assigned for the different groups of analysis, so pups of the same litter were included in different groups of analysis, (maximum two female or male pups were chosen) (Table 1). Cohort I, male and female Wistar rats, controls and A1254 exposed, were assigned to three groups of analysis: brain tissues were analyzed for immunofluorescence for AVP (n = 15 males, 13 females); endpoint RT-PCR analysis of cFOS, (n = 12 males, 12 females), and in situ hybridization for AVP (n = 14 males, 20 females). All groups included four treatment conditions: euhydrated rats (Control) and exposed to A1254; salt-loaded control rats (Hyper) and exposed (Hyper + A1254). Special care was taken to make sure that all female rats in the different groups were in the same phase of the estrous cycle. Cohort II, adult male SD rats (n = 18) were processed with immunoperoxidase to stain AVP as previous report (Khan et al., 2000). This group included four treatment conditions: euhydrated rats (Control) and exposed to A1254; with acute hyperosmotic challenge control (Hyper) and exposed (Hyper + A1254) rats. Cohort III, Wistar male rats (n = 15), were processed for immunofluorescence to stain AVP. This group included rats euhydrated control and exposed to DE-71; salt-loaded control (Hyper) and exposed (Hyper + DE-71), (see Table 1).

2.4. Prolonged osmoregulatory challenge (salt loading)

To determine if perinatal exposure to A1254 or DE-71 alters AVP content and synthesis in the PVN and SON of euhydrated and physiologically activated animals, a subset of A1254 and DE-71-treated or control rats (from each cohort) were exposed to a chronic hyperosmotic challenge. It was carried out by replacing their drinking water with 2% saline solution (20 g NaCl/l; ad libitum access) for 5 days, as previously described (Curras-Collazo and Dao, 1999; Amaya et al., 1999). Rats were weighed before and after the hyperosmotic challenge. They were considered dehydrated when they lost about 10% of their body weight (data not shown). These were labeled as hyperosmotic rats (Hyper). Euhydrated (normosmotic) rats (control and treated) had ad libitum access to tap water.

2.5. Acute osmoregulatory challenge

To determine whether perinatal A1254 exposure had effects on AVP immunoreactivity after acute hyperosmotic challenge, a group of SD male offspring 3–5 months old (n = 18) was used. Male offspring were injected intraperitoneally (ip; 0.6 ml NaCl/100 g b.w.) with either 3.5 M NaCl (Hyperosmotic solution) or 0.154 M NaCl (0.9% NaCl isotonic solution; Control) and animals were sacrificed 4–4.5 h later as described (Ludwig et al., 1994; Coburn et al., 2015). This manipulation has been shown to produce marked stimulation of somatodendritic AVP release (Coburn et al., 2015; Ludwig et al., 1994). Tail blood was collected before sacrifice and plasma osmolality was measured to confirm increased plasma osmolality in Hyper rats of 5.0% or greater.

2.6. Tissue processing

Upon completion of the osmotic challenge, all rats were anesthetized with sodium pentobarbital (63 mg/kg). They were transcardially perfused with a clearing solution (150–200 ml of 0.9% saline containing 2500 IU/500 ml heparin (PISA Farmacéutica Mexicana Mex.) followed by 350–400 ml of 4% paraformaldehyde (Sigma Chemical Co., St. Louis, MO) in PBS (0.1 M phosphate-buffered saline, pH 7.4). Brains were removed and postfixed in the same fixative at 4 °C for 2 h. They were then cryoprotected in 30% sucrose and stored at 4 °C until used. Coronal slices (30 μm) through the hypothalamic PVN and SON (Bregma: −0.80

Table 1
Cohort distribution, rat strains used, dosing pattern pups used, and testing paradigm.

Cohort	Dams/pups (used)	Chemical and doses	Osmotic challenge	Treatment groups	Osmolality	AVP-IF or AVP-IP	AVP-mRNA ISHH	cFOS mRNA RT-PCR
I	Wistar 25/86	A1254 30 mg/kg/day orally GD: 10–19	Euhydrated (Tap water)	Control	8 M, 4 F	15 M,13 F	14 M, 20 F	12 M,12 F
				A1254	8 M, 4 F	Section 2.8, Section 2.11	Section 2.12	Section 2.13
			Prolonged (Salt Loading) Section 2.4	Hyper	10 M, 3 F	Stat: 2-way ANOVA	Stat: 2-way ANOVA	Stat: 2-way ANOVA
				Hyper + A1254	9 M, 4 F			
II	SD 8/18	A1254 30 mg/kg/day orally GD: 10–19	Euhydrated (0.154 M NaCl sol. i.p.)	Control	5 M	18 M		
				A1254	4 M (No data)	Section 2.9		
			Acute (3.5 M NaCl sol. i.p.) Section 2.5	Hyper	4 M	Stat: 1-way ANOVA		
				Hyper + A1254	5 M			
III	Wistar 10/15	DE-71 30 mg/kg/day orally GD: 6 to PND 21	Euhydrated (Tap water)	Control	4 M, 4 F	15 M		
				DE-71	3 M, 7 F	Section 2.8, Section 2.11		
			Prolonged (salt loading) Section 2.4	Hyper	4 M, 3 F	Stat: 1-way ANOVA		
				Hyper + DE-71	4 M, 6 F			

Table shows cohort distribution, strain of rats, dosing pattern, number of offspring used, treatment groups, and testing paradigm for the perinatal exposure to commercial Aroclor 1254 (A1254) or PBDE (DE-71) mixtures (30 mg/kg/day, orally). For A1254, the exposure was from gestational day (GD) 10 to 19. For DE-71, the exposure started at GD 6 and continued through postnatal day (PND) 21. At 3–5 months of age (250–450 g), before sacrifice, some male and female rats from control and A1254 or DE-71 exposed were subjected to a prolonged (NaCl 2% drinking solution during 5 days ad libitum) or acute (ip; 3.5 M NaCl) osmotic challenge. Pups were randomly assigned for the different groups of analysis. For cohort I: vasopressin immunofluorescence (AVP-IF), AVP-mRNA in situ hybridization histochemistry (ISHH) and cFOS-mRNA final point reverse transcription polymerase chain reaction (RT-PCR). For cohort II: AVP immunoperoxidase (AVP-IP). For cohort III: AVP-IF. The paradigms included four treatments groups: euhydrated (Control) and exposed (A1254 or DE-71) rats, salt-loaded control (Hyper) and exposed (Hyper + A1254 or DE-71) rats. All groups included plasma osmolality measurements.

to −2.12 mm) (Paxinos and Watson, 1998) were cut on a sliding-freezing microtome (Leitz, Grand Rapids, MI) and collected in plastic wells containing PBS. Serial sections were placed alternately in six wells containing eight cuts per well approximately. Each well had a set (eight slices) of all representative rostrocaudal PVN and SON. Free-floating sections from three sets were processed for immunohistochemistry.

2.7. Osmolality

Under anesthesia and prior to perfusion, 2 ml cardiac blood samples were collected from each rat and centrifuged at 8000 rpm for 5 min. Osmolality was measured in triplicate with a vapor pressure osmometer (Wescor 5500, Logan, UT). Results for osmolality are reported as mean ± s.e.m. in mOsm/kg units.

2.8. Immunofluorescence for AVP

Immunofluorescence was carried out in Wistar rats from cohorts I and III that included four treatment groups for A1254: Control (n = 4 males, 3 females), A1254, (n = 3 males, 3 females), Hyper (n = 5 males, 4 females), and Hyper + A1254 (n = 3 males, 3 females). For DE-71 (male rats): Control (n = 4), DE-71 (n = 3), Hyper (n = 4), and Hyper + DE-71 (n = 4) (see Table 1). The sections containing anterior, middle, and posterior hypothalamic PVN and SON regions were processed simultaneously for all groups of each A1254 or DE-71 studies. They were incubated in blocking solution containing 5% normal donkey serum, 5% BSA, and 0.3% Triton X-100, for 60 min at room temperature to minimize nonspecific staining. Then, the sections were incubated with vasopressin-neurophysin antibody (PS-41 monoclonal, gifted by H. Gainer, NIH) (Ben-Barak et al., 1985; Whitnall et al., 1985) at a 1:200 dilution in blocking buffer containing 1% teleostean gelatin (Sigma Chemical Co., St. Louis, MO), for 48 h at 4 °C in free flotation with continuous shaking. The sections were then washed for three times for 10 min each in PBS-T (PBS with 0.3% Triton X-100) followed by a 1.5 h incubation with Alexa Fluor 488 donkey anti-mouse secondary antibody (Invitrogen Corp., Carlsbad, CA) at 1:200 dilution in blocking solution, in a humidified chamber at 37 °C. Afterward, the sections were washed (3 × 10 min) in PBS and mounted onto glass slides with an anti-fade mounting medium (ProLong Antifade Kit, Molecular Probes; Eugene, Oregon USA). For several sections obtained from each group, the primary antibody was replaced by blocking solution representing methodological control sections. Staining observed in these sections was used in background correction as part of computer-assisted densitometry (see below). The structures in the immunohistochemical control sections in which the fluorescence was not observed were considered immunoreactive to AVP. The sections were analyzed with a Zeiss 510 META laser scanning confocal microscope, equipped with a 488-nm argon-ion laser (Alexa Fluor 488 dye) attached to an Axiovert 200 M microscope. They were analyzed with a 10× Plan-Neofluar NA = 0.3 and a 20× Plan-Neoufluar NA = 0.5 Objective (Carl Zeiss). Before analyzing the sections, we conducted a lambda stack to obtain the emission spectrum of this fluorophore. Barrier filters were placed to obtain only the peak fluorescence emission. Images from each section (30 μm thickness) were acquired and analyzed bilaterally on the optimal focal plane, in single track mode, with the Ar laser/488 nm, pinhole diameter (1 airy unit) and detector gain (1). Laser power was adjusted to provide an optimal dynamic range for the measurements (the same in all slides). Confocal images were converted to an 8-bit TIF format with a Zeiss LSM image browser (v 3.5).

2.9. Immunoperoxidase for AVP

After acute hyperosmotic challenge, animals were fixed as above (4% paraformaldehyde). Coronal brain sections (40 μm) of perinatal A1254 exposed male Sprague-Dawley rats (n = 18), were processed with immunoperoxidase to stain AVP. The technique was carried out as previously reported (Khan et al., 2000). Briefly, brain sections were mounted on gelatin-subbed glass slides. In each experiment control sections received all solutions except the primary antibody (methodological control). Sections on slides were washed in PBS and treated with blocking/permeabilization solution (0.2% gelatin, 0.3% Triton-X, 0.4% BSA) for 30 min. Tissue was incubated with an AVP antibody PS41, dilution 1:100. After wash, the sections were incubated with an anti-mouse secondary antibody (Dako; K4001). AVP immunoreactivity was developed in nickel intensified 3,3′-Diaminobenzidine solution. Sections were dehydrated in an alcohol series and coverslipped using DPX mounting medium (Electron Microscopy Sciences), later analyzed using bright field microscopy and images were taken of PVN and SON (3–7 images per nucleus per rat) using a digital camera (Spot Insight Meyer).

2.10. Image analysis

All images were analyzed for integrated optical density (IOD) using computer-assisted densitometry software (Image Pro Plus 4.5, Media Cybernetics, MD, USA). Images were converted to a gray scale (0–255) and their background was subtracted. Subsequently, the IOD of the immunoreactivity was quantified for the area of interest. The PVN and the SON areas were manually outlined in at least six sections per nucleus per rat. Integrated density values (density × area) were determined per section for each nucleus. The IOD was reported as arbitrary units. Average IOD was obtained for each regions of interest (bilateral PVN and bilateral SON) by pooling IOD values of rats in respective experimental groups.

2.11. Cell count analysis of AVP-IR neurons

To determine if A1254 or DE-71 exposure affected the number of vasopressinergic neurons or only the intensity of AVP immunoreactivity (measured with an IOD analysis), we counted the AVP immunoreactive (AVP-IR) neurons in PVN and SON for all male groups (cohort I, III). We selected 3–5 immunofluorescent micrographs, of PVN and SON—only the medial portions—for each animal in each group, for IOD quantification (Bregma: −1.80 mm to −1.88 mm for PVN and −1.30 mm to −1.40 mm for SON) (Paxinos and Watson, 1998). Neurons with evident nuclei and AVP immunoreactivity were considered. To avoid counting the same neurons more than once, we overlaid a grid with square sections (24.5 × 24.5 μm) on the images and counted the cells that were marked with a X. For this analysis, we used Image-J software with the plugin analyzer-cell counter (v 1.44p, National Institute of Health, available at http://imagej.nih.gov/ij).

2.11.1. Cell count analysis of Nissl staining. In addition to analyze the possible changes in the overall cell density we counted the total number of cells in the above-mentioned medial portions of the PVN and the SON in Nissl-stained sections of normosmotic control and A1254- and DE-71-exposed adult male rats. The brains of four control and three A1254- or DE-71-exposed rats were fixed and collected as previously described. For Nissl staining, coronal brain slices (30 μm thick) were mounted on gelatin-coated slides and dried overnight. The sections were immersed in a solution (100 ml) containing cresyl-violet (0.5%), sodium acetate (2.7%), and glacial acetic acid (0.92%), for 2 min. Then, sections were dehydrated through a series of graded ethyl alcohols (70%, 80%, 96%, each for two minutes; 100% twice for two minutes), cleared in xylene twice (5 min), and cover-slipped with Entellan resin (Merck, Germany). Cells were counted with the aforementioned procedures.

2.12. In situ hybridization histochemistry (ISHH)

We conducted in situ hybridization to determine the anatomical distribution of AVP mRNA and to determine the effect of perinatal

exposure to A1254 on the synthesis of AVP in euhydration or in response to hyperosmotic activation. Male and female rats perinatally exposed to A1254 or vehicle, were allowed to mature to 3 months of age, and randomly assigned to four experimental groups: 1) control (n = 4 males, 5 females), 2) A1254 (n = 3 males, 5 females), 3) Hyper (n = 3 males, 4 females) and 4) Hyper + A1254 (n = 4 males, 6 females). Both control and exposed rats were randomly selected to be dehydrated. The fixed tissue (4% paraformaldehyde) was processed in the same way as for immunohistochemistry (see above), except that materials and solutions were RNAse free. A series of 18-μm thick coronal sections were cut through the rostrocaudal extent of the PVN and the SON on a cryostat (Microm HM525, GmbH, Germany). Every fourth section cut through the PVN or the SON was collected and mounted onto Superfrost/Plus glass slides to obtain four sets for each PVN and SON. Sections were desiccated overnight at 42 °C and stored at −80 °C until processed for in situ hybridization histochemistry.

2.12.1. AVP probe for ISHH. The 200 bp-DNA fragment containing AVP was amplified by PCR using male or female rat cDNA from the PVN as a template. Two oligonucleotides were chosen using the Primer3 (v. 0.4.0) software [http://bioinfo.ut.ee/primer3-0.4.0/primer3/] with an introduction of a restriction enzyme site for posterior steps of subcloning. Sense SHindIII 5′- TCA GTC **AAG CTT** CAC CTC TGC CTG CTA CTT C -3′, which introduced a *Hin*dIII restriction site (bold), and Antisense *Eco*RI 5′- TAC TAT **GAA TTC** GGG GTA CAG GTT CTC CTC C -3′, which introduced an *Eco*RI site (bold). The PCR conditions were 27 cycles at 94 °C - 1 min, 64 °C − 1 min, 72 °C − 1.15 min, and a final cycle at 72 °C − 10 min.

The resulting PCR product was extracted and purified with the High Pure PCR Product Purification Kit (Roche, Mannheim, Germany). The purified fragment was cloned into the pJET1.2/blunt vector from CloneJET™ PCR Cloning Kit (Fermentas) as specified by the manufacturer, with the ligation reaction at 22 °C for 20 min. The ligation mixture was electro-transformed using 50 μl of electrocompetent DH5α cells and was incubated at 37 °C for 1 h. Subsequently, the electroporated cells were poured into Petri dishes containing 2xYT medium and ampicillin (200 mg/ml final concentration) and were incubated at 37 °C for 12 h.

To select positive colonies containing the vector and vasopressin fragment, we performed a colony PCR using SHindIII and AsEcoRI and the above-described PCR conditions. Plasmids of selected colonies were isolated according to a standard alkaline lysis protocol, and single-pass sequencing of the 5′-termini was conducted with the pJET1.2 Forward Sequencing Primer (5′-CGA CTC ACT ATA GGG AGA GCG GC-3′) and an automated analyzer (Model 3100, Applied Biosystems, Foster City, CA), as specified by the manufacturer.

The pJET plasmid containing vasopressin was digested with the *Hin*dIII and *Eco*RI restriction enzymes, and the released fragment was extracted from agarose gel and subsequently purified using the High Pure PCR Product Purification Kit. The purified fragment was ligated into a pSPT18 vector (Roche, Cat. 10,999,644,001), previously digested with *Hin*dIII and *Eco*RI enzymes, using T4 DNA ligase, as per the instructions of the manufacturer. The ligation was electroporated into electrocompetent DH5α cells, and plasma DNA from four colonies was sequenced using SHindIII and AsEcoRI to confirm the presence of the insert containing AVP. Transcripts obtained from the four clones gave the expected mRNA distribution pattern for AVP in the CNS when used as a probe for ISHH (not shown).

2.12.2. ISHH technique. Every fourth section of the PVN and the SON was hybridized with a 200-bp single-stranded α [^{35}S] UTP-labeled RNA probe, complementary to the coding region of the rat AVP gene (47 to 247 nucleotides of the cDNA; GenBank: M25646.1). Hybridization was performed as previously described (Sanchez et al., 2009). The tissues were pre-treated in 50% formamide/2× SSC. The hybridizations were performed in a buffer containing 50% formamide, 2× SCC, 10% dextran sulfate, 1× Denhardt's [0.25% BSA, 0.25% Ficoll 400, 0.25% polyvinylpyrrolidone], 0.25% 1 M Tris-HCl pH 8.0, 5% sodium dodecyl sulfate, 250 μg/ml denatured salmon sperm DNA, and a 5×10^5 cpm radiolabeled probe at 54 °C for 16 h. Slides with hybridized brain sections were dipped into Kodak NTB autoradiography emulsion (Eastman Kodak) diluted 1:1 in distilled water. These slides were developed after 4 days of exposure at 4 °C. Developed silver grains analyzed from the hybridized slides were visualized under dark-field illumination (Olympus BX51, 10×/0.3 NA objective). Images were obtained with a SPOT II digital camera (Diagnostic Instruments, Inc.), the areas of interest (PVN and SON) were outlined. IOD values were estimated in each section with background correction (as background the adjacent tissue without AVP mRNA signal was taken). The specificity of the signal was demonstrated in hybridized tissue using the sense probes. Blind quantitative analysis was performed independently by two observers, without major differences among them. The average of the IOD values of up to six rostrocaudal slices/animal was calculated, treated as one determination, and was used to estimate the mean and s.e.m./group. Two different repetitions were performed and analyzed twice by independent ISHH trials on different sets of sections, giving similar results.

2.13. Endpoint reverse transcription polymerase chain reaction (RT-PCR)

Endpoint RT-PCR to cFOS gene expression was performed to determine if the PVN and SON of A1254 perinatally exposed rats are activated in response to hyperosmotic challenge. We used three-month-old rats, 12 females and 12 males (Control, A1254, Hyper, Hyper + A1254; n = 3 rats per sex per group). Upon completion of the osmotic challenge, the rats were killed by rapid decapitation with a guillotine, and trunk blood was collected to determine plasma osmolality. The brains were rapidly removed from the skull, placed on dry ice, and stored at −80 °C until use. Brains were sectioned on a cryostat until reaching the beginning of the regions of interest, taken out on dry ice and cut frozen into a thick coronal section in a range of −1.30 to −2.12 mm for the PVN and −0.80 to −1.80 mm for the SON caudal to Bregma (Paxinos and Watson, 1998). The PVN and the SON were punched out of the tissue using the micropunch technique (Palkovits, 1988) and kept frozen in a tube on dry ice. Total RNA was extracted as described (Chomczynski and Sacchi, 1987), and RNA concentration was determined by absorbance at 260 nm. Only samples with a 260/280 nm ratio of >1.8 and >2.0 28S/18S ratio, verified by gel electrophoresis in 1% agarose -1× TBE, were used. One microgram of RNA was transcribed with M-MLV reverse transcriptase and oligo-dT. The 18S was used as reference gene. PCR reactions were performed as follows, 1336–1553 of 18S ribosomal RNA (rRNA) cDNA (GenBank: X01117.1); final product: 218 bp; sense: 5′- ATGGCCGTTCTTAGTTGGTG -3′, antisense: 5′- CGCTGAGCCAGTTCAGTGTA -3′. For cFOS cDNA, sense: 5′ -CAATACACTCCATGCGGTTG -3′, antisense: 5′ – CCCGTAGACCTAGGGAGG AC-3′. To ensure adequate conditions for the semi-quantification of mRNA expression for each probe, cDNAs prepared from 1.0 μg of RNA in the PVN and SON were subjected to PCR amplification cycles (Mastercycler, Ependorff, Hamburg, Germany). The number of cycles for each cDNA was obtained from the ascending part of the curve that plots optical density versus number of PCR cycles. 18S rRNA: 2 μl of cDNA per 25 μl PCR [94 °C 1′15″, 65 °C 1′, 72 °C 1′] × 30 cycles + 15 min at 72 °C for a final extension. cFOS: 2 μl of cDNA per 25 μl PCR [94 °C 1′15″, 60 °C 1′, 72 °C 1′] × 32 cycles + 15 min at 72 °C for a final extension. Products were separated by gel electrophoresis in 2% agarose -1× TBE, running buffer (0.5×), and stained with ethidium bromide; density was quantified with a Fluor-S MultiImager (BioRad). Samples of control and experimental animals from the same group were included in the same gel. The relative values for cFOS mRNA were estimated as the ratios of mRNA signal to 18S rRNA signal.

2.14. Statistical analysis

Statistical significance between groups was determined by one or two-way ANOVA depending on the factors tested. For two-way ANOVA the factors tested were sex and treatment, while data from males was assessed with one-way ANOVA (treatment). Where overall significance was obtained ($p < 0.05$), post-hoc comparisons were made using Holm-Sidak method. Results for osmolality are reported as mean ± s.e.m. in mOsm/kg units. Average values from each cohort were statistically analyzed in an independent way using two-way ANOVA for cohort I and III and one-way ANOVA for cohort II.

For AVP immunofluorescence and immunoperoxidase, the mean IOD values were tested with two-way ANOVA (cohort I), and one-way ANOVA (cohort II, III). For cell counting, averages of immunoreactive neurons from cohort I and III were evaluated with one-way ANOVA. Nissl-stained neurons were analyzed using one-way ANOVA. For ISHH, the mean IOD values were tested with two-way ANOVA (cohort I). For endpoint reverse transcription polymerase chain reaction (RT-PCR), the statistical significance between groups was determined by two-way ANOVA (cohort I). Statistical analysis was performed using SigmaPlot 12.3 (Systat Sofware, Inc). ANOVA was performed where data met normality and homogeneity of variance assumptions. Statistical significance was acknowledged at an alpha level of 0.05.

3. Results

3.1. Perinatal A1254 and DE-71 treatment affect osmoregulatory capacity during hyperosmotic challenge in adulthood

Cardiac blood was collected and analyzed for plasma osmolality (Table 2) from the three cohorts. Plasma responses were measured in normosmotic conditions: corn-oil vehicle (Control); A1254 (A1254) or DE-71 (DE-71) exposed, and in rats subjected to prolonged or acute hyperosmotic challenge: corn-oil vehicle (Hyper); exposed to A1254 (Hyper + A1254), or DE-71 (Hyper + DE-71). In all cohorts plasma osmolality data showed an expected elevation in response to hyperosmotic stimulation. Cohort I (males and females perinatal exposed to A1254 and subjected to prolonged hyperosmotic challenge) was evaluated with two-way ANOVA (sex and treatments). Plasma osmolality values were not significant differences between sexes ($F_{1,147} = 1.56$, $p = 0.21$); there was no interaction between sex and treatment ($F_{3,147} = 0.77$ $p = 0.51$). There was a statistically significant difference in the mean omoslality values between the treated groups ($F_{3,147} = 9.17$, $p < 0.001$). Post-hoc multiple comparison testing showed that Hyper and Hyper + A1254 group had a significant increase in plasma osmolality relative to normosmotic controls ($p = 0.002$, $p < 0.001$ respectively). Hyper + A1254 group showed a significant increase in plasma osmolality relative to A1254 group ($p = 0.035$).

Cohort II (males perinatally exposed to A1254 and subjected to acute hyperosmotic challenge) was evaluated using one-way ANOVA. It showed significant differences between treatment groups ($F_{2,13} = 12.6$, $p = 0.001$). Multiple comparison revealed that both Hyper ($p = 0.012$) and Hyper + A1254 ($p = 0.001$) groups had a significant increase in plasma osmolality relative to control.

Cohort III (DE-71 perinatal exposure and subjected to prolonged hyperosmotic challenge) was evaluated with two-way ANOVA. Plasma osmolality values were not significant different between sexes ($F_{1,94} = 1.04$, $p = 0.31$), but there was a significant sex and treatment interaction ($F_{3,94} = 4.31$ $p = 0.007$). There were statistically significant differences in the mean osmolality values between the treated groups ($F_{3,94} = 54.4$, $p < 0.001$). Post-hoc multiple comparison testing showed that Hyper males and females had a significant increase in plasma osmolality relative to normosmotic controls ($p < 0.001$). Female Hyper + DE-71 rats showed a significant increase in plasma osmolality relative to DE-71 normosmotic control ($p < 0.001$). A similar tendency was seen in males but the effect was not statistically significant ($p = 0.11$). Additionally, in both sex groups, Hyper + DE-71 rats showed significant lower plasma osmolality relative to Hyper group ($p < 0.001$). There were not differences between males and females within control, Hyper and Hyper + DE-71 groups ($p > 0.05$), but there was a significant sex difference within the DE-71 treatment ($p = 0.011$). In combination these findings may indicate aberrant osmotic activation and/or dysregulation induced by developmental exposure to PBDEs in male and female adult Wistar and SD rats.

3.2. Perinatal exposure to A1254 prevents the AVP physiological response to hyperosmotic challenge

3.2.1. AVP immunofluorescence. Image analysis of coronal brain sections from the PVN and SON of male and female rats perinatally exposed to A1254 and subjected to prolonged hyperosmotic challenge (cohort I) shows that in control groups (vehicle) AVP-IR is mainly in MNCs. Basal AVP-IR was abundant and uniformly distributed in soma and fibers emanating from these nuclei (Fig. 1A, E). Perinatal exposure to A1254 leads to increase the AVP-IR in PVN compared to control group (Fig. 1B, F). Prolonged hyperosmotic stimulation (Hyper) showed an expected physiological increase of AVP-IR relative to control groups. These differences are notable in MNCs cytoplasm and in some parvocellular cell

Table 2
Plasma osmolality (mOsm/kg) in adult rats perinatally exposed to A1254 or DE-71 and in response to prolonged or acute hyperosmotic challenge.

Cohort	Experimental conditions			Hyperosmotic challenge			
				Prolonged		Acute	
	PCBs	Control	A1254	Hyper	Hyper + A1254	Hyper	Hyper + A1254
I	W. Males + Females	303.3 ± 4 n = M8, F4	324.8 ± 4.8 n = M8, F4	331.8 ± 5** n = M10, F3	346.4 ± 4.9^*** n = M9, F4		
II	SD. Males	297.3 ± 1.7 (n = 5)				329.1 ± 4.4** (n = 4)	340.4 ± 9.6*** (n = 5)
	PBDEs	Control	DE-71	Hyper	Hyper + DE-71		
III	W. Males	307.2 ± 2.0 (n = 4)	306.3 ± 2.3 (n = 3)	333.7 ± 4.7*** (n = 4)	314.8 ± 1.9### (n = 4)		
	W. Females	313.3 ± 1.9 (n = 4)	299 ± 2.0† (n = 7)	336.3 ± 2.7*** (n = 3)	320.9 ± 1.9^^^### (n = 6)		

Table shows osmoregulatory capacity measured during normosmotic and hyperosmotic conditions in Wistar (W) or Sprague Dawley (SD) adult rats (3–5 months old) perinatally exposed to A1254 or DE-71 (30 mg/kg/day orally) or corn-oil vehicle (Control). Rats from these groups were subjected to prolonged hyperosmotic challenge (NaCl 2% drinking solution during 5 days ad libitum) or acute osmotic challenge (NaCl 3.5 M *i.p.*), (Hyper; Hyper + A1254 or Hyper + DE71groups). Under anesthesia, blood was collected at sacrifice. Plasma osmolality was measured and the values are expressed as mean ± s.e.m. in mOsm/kg. Average values from each cohort were statistically analyzed independently using two-way ANOVA for cohort I and III and one-way ANOVA for cohort II, followed by post-hoc comparisons using the Holm-Sidak method. For the plasma osmolality values from cohort I, there were no significant interactions between sexes and between sex and treatment. This is the reason that it is depicted as a single group. Symbols indicates significant differences as determined by one or two-way ANOVA. Asterisks (*) compared to control, number symbols (#) compared to Hyper, carets (^) compared to A1254 or DE-71 treatment and daggers (†) compared to the other sex ($p < 0.05$ = ^,†, $p < 0.01$ = **, ##, $p < 0.001$ = ***, ###, ^^^).

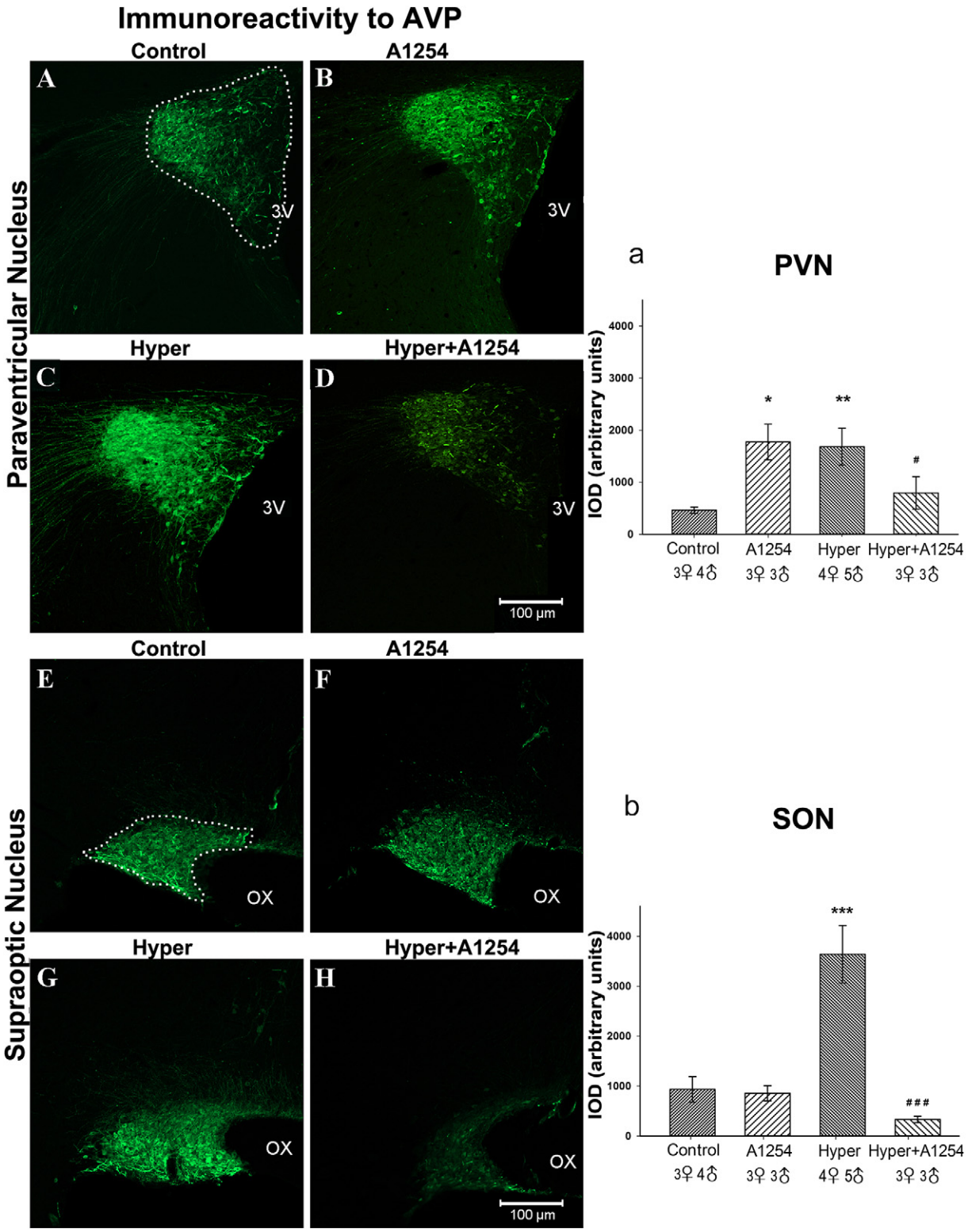

Fig. 1. Effects of perinatal exposure to Aroclor 1254 (A1254) on AVP immunoreactivity (AVP-IR) in 3-month-old Wistar rats. LEFT: Panel of representative confocal images from male rats of PVN and SON coronal sections with AVP-IR: control rats (images A and E); A1254-treated rats (30 mg/kg/day) (images B and F); hyperosmotic salt-loaded rats (Hyper) (images C and G); and hyperosmotic A1254-treated rats (Hyper + A1254; D and H). There was an increase in AVP-IR in Hyper rats (C and G). In contrast, there was an evident decrease in immunoreactive intensity and number of AVP-IR neurons and fibers after A1254 exposure (Hyper + A1254; D and H). RIGHT: The graphs show the effects of A1254 on AVP-IR integrated optical density (IOD) in the PVN (a) and the SON (b) from males and females. There were no significant differences between sexes and no interactions between sex and treatment. This is the reason that it is depicted as a single group. The dotted line shows the ROI used to perform IOD measurements. The bars represent mean values ± s.e.m. The symbols represent statistical significance as determined by two-way ANOVA and Holm-Sidak post-hoc tests. Asterisks (*) compared to control and number symbols (#) compared to Hyper ($^{*,\#} = p < 0.05$; $^{**} = p < 0.01$; $^{***\#\#\#} = p < 0.001$). Abbreviations: third ventricle (3V); optic chiasm (OX); Bar = 100 µm.

bodies and their long vesiculated fibers (Fig. 1C, G). In contrast, the intensity of AVP-IR and the amount of the AVP-IR cells were lower in the PVN and SON from the Hyper + A1254 group as compared to the A1254 and to the Hyper groups (Fig. 1D, H). These observations were corroborated with semiquantitative analysis of the AVP-IR density (Fig. 1a, b), evaluated with two-way ANOVA (sex and treatment).

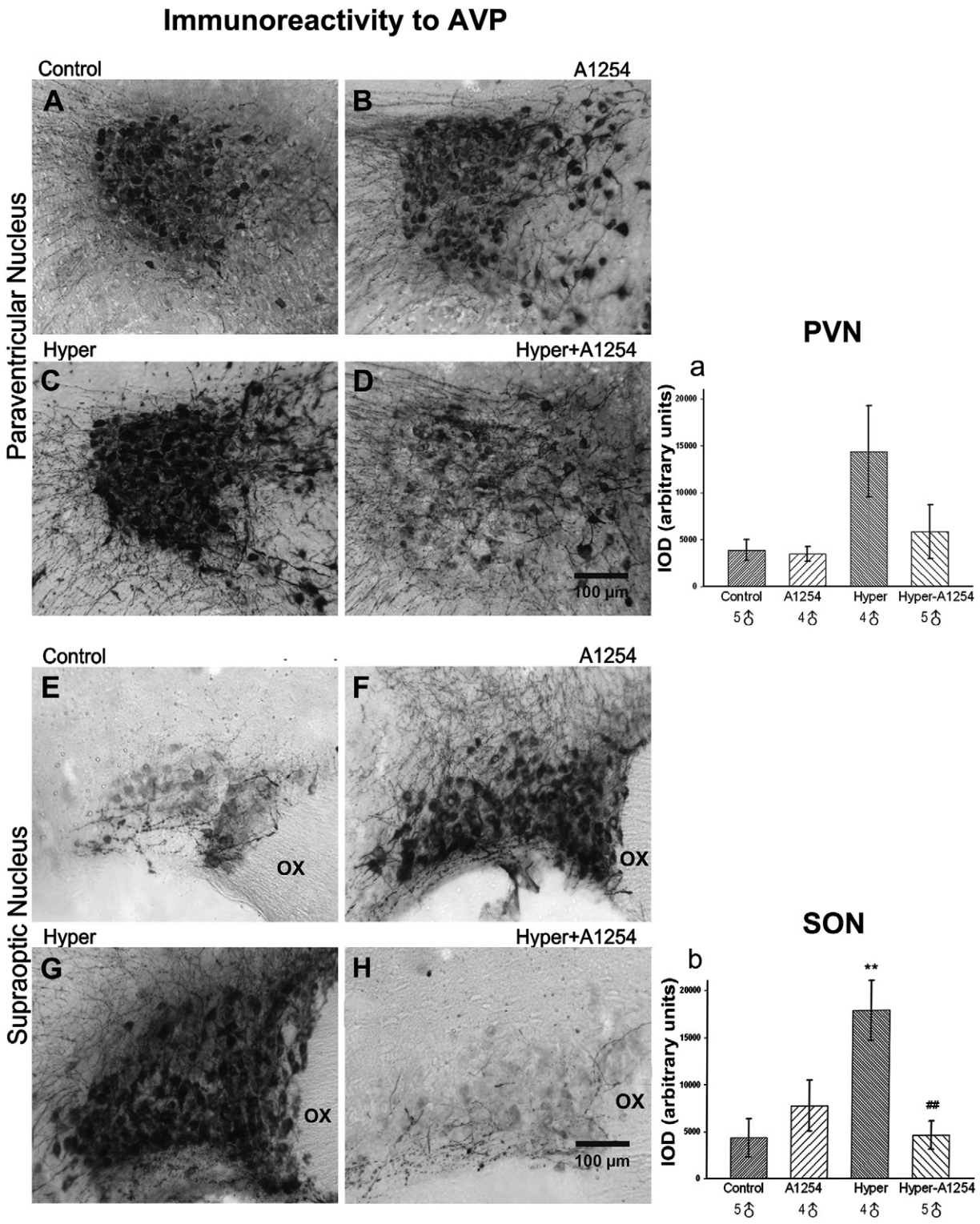

Fig. 2. A1254 prevents upregulation of AVP-IR in response to acute osmotic activation in the SON and PVN of male Sprague-Dawley rats perinatally exposed to Aroclor 1254 (A1254; 30 mg/kg/day). LEFT: Representative micrographs were generated using AVP immunoperoxidase in PVN and SON sections. Control (vehicle) images A and E; A1254-treated rats B and F; rats subjected to an acute hyperosmotic challenge (Hyper; 3.5 M NaCl; 0.6 ml/100 g body weight, *i.p.*) images C and G; and hyperosmotic A1254-treated rats (Hyper + A1254; D and H). There was an increase in AVP-IR in Hyper rats (C and G). In contrast, there was a marked reduction in upregulation of immunoreactive intensity and distribution of AVP-IR neurons and fibers in Hyper + A1254 group (D and H). RIGHT: Bars show mean ± s.e.m. values of AVP-IR IOD in PVN (a) and SON (b). Symbols represent statistical significance as determined by one-way ANOVA and Holm-Sidak post-hoc tests. Asterisks (*) compared to control, number symbols (#) compared to Hyper (**, $^{\#\#} = p < 0.01$). Abbreviations: optic chiasm (OX); Calibration bar = 100 µm.

Mean IOD values were not significantly different between sexes in the PVN ($F_{2,63} = 3.18$, $p = 0.08$) nor in the SON ($F_{1,60} = 3.75$, $p = 0.05$). Neither was significant interaction between sex and treatments in the PVN ($F_{3,63} = 2.08$, $p = 0.11$) or SON ($F_{3,60} = 1.38$, $p = 0.25$). As expected, there were significant differences between the treatments groups, both in the PVN ($F_{3,63} = 6.05$, $p = 0.001$) and SON ($F_{3,60} = 18.56$, $p < 0.001$). Multiple comparison indicated significant differences when comparing A1254 group with control group from PVN ($p = 0.012$). Mean IOD values from the Hyper groups showed statistically significant increases compared to controls in PVN ($p = 0.004$) and in the SON ($p < 0.001$). In contrast, the mean IOD for the Hyper + A1254 groups was not different from the controls. When comparing Hyper + A1254 to the Hyper groups they have a significant IOD decrease, (PVN $p = 0.047$; SON $p = 0.001$; Fig. 1a, b). In the PVN, the comparison of Hyper group versus Hyper + A1254, shows a reduction in the mean IOD values of 74.7% in males and 67.08% in females. In the SON this comparison showed a reduction in mean IOD values of the 95% in males and 86.24% in females.

3.2.2. AVP immunoperoxidase. AVP immunostaining in PVN and SON sections of cohort II (adult males perinatally exposed to A1254 and subjected to acute dehydration) showed similarly decreased AVP-IR responses to acute hyperosmotic stimulation when compared to rats that were chronically activated (Fig. 2). First, AVP-IR was uniformly distributed in soma and fibers of MNCs in PVN and SON. A1254 treated rats had similar AVP-IR to controls in both nuclei. As in Cohort I Hyper rats showed more robust AVP-IR as compared to the control group. Upregulated AVP-IR responses in the Hyper + A1254 group were not observed when compared to A1254 and Hyper groups both in PVN and SON. Mean IOD values for AVP-IR were evaluated using one-way ANOVA. In the PVN there were not significant differences between groups ($F_{3,14} = 3.10$, $p = 0.061$). In the SON there were significant effects between treatment groups ($F_{3,14} = 6.29$, $p = 0.006$). Multiple comparison showed that mean IOD values from Hyper group were significantly greater compared to control ($p = 0.011$). When comparing Hyper versus Hyper + A1254, IOD values decreased significantly ($p = 0.011$; Fig. 2a and b).

3.2.3. AVP-IR in DE-71-exposed male rats. Brain sections of control normosmotic groups have a medium intensity (basal) AVP-IR in the PVN and the SON, mainly in MNC cell bodies (Fig. 3A, E). Sections from DE-71-treated rats showed an increase in basal AVP-IR in PVN and SON (Fig. 3B, F). Sections from Hyper rats showed an evident physiological AVP-IR increase in MNCs and parvocellular neurons in the PVN and in MNCs of the SON (Fig. 3C, G). Hyper + DE-71-treated rats did not show this increase; rather, they had weak AVP-IR in the PVN and the SON (Fig. 3D, H). Also the number of AVP-IR neurons was reduced, finding confirmed by cell count analysis (Fig. 4C, D). Mean IOD values for AVP-IR are shown in the graphs of Fig. 3(a, b). The differences of the mean IOD values for AVP-IR between the treatment groups were evaluated using one-way ANOVA, Indicating significant differences both in the PVN and SON ($F_{3,40} = 10.9$, $p < 0.001$ and $F_{3,45} = 14.54$, $p < 0.001$ respectively). Multiple comparison showed, in the SON, that the IOD values from DE-71 treated group were significantly different compared to the control group ($p = 0.021$). The Hyper groups from PVN and SON showed statistically significant increases compared to controls ($p < 0.001$ both). In contrast, the mean IODs for the Hyper + DE-71 groups were not different from the controls. The Hyper + DE-71 group showed a significant decrease in the SON ($p = 0.026$), when compared with its own control, the DE-71 group. When compared Hyper with Hyper + DE-71 groups, the mean IOD decreased significantly in both PVN and SON ($p < 0.001$ both; Fig. 3a, b). These comparisons showed a reduction in mean AVP-IR IOD values of the 88.24% in the PVN, and 77.03% in the SON.

3.3. Cell count analysis of AVP-IR neurons

A cell count analysis was performed with same immunofluorescence images acquired from cohorts I and III male rats. Only the photographs from the middle part of the PVN and the SON were used (Bregma: −1.80 mm to −1.88 mm for the PVN, and −1.30 mm to −1.40 mm for the SON) (Paxinos and Watson, 1998). Cell counts included all AVP-IR MNCs and parvocellular neurons. One-way ANOVA indicated significant differences between treatment groups in the number of AVP-IR neurons by A1254 treatment in PVN ($F_{3,70} = 5.35$, $p = 0.002$) and SON ($F_{3,45} = 22.14$, $p < 0.001$). Multiple comparisons showed that in A1254-treated rats, the number of the AVP-IR neurons in the PVN and SON were not significantly different compared to its control (Fig. 4A, B). The Hyper groups had a significantly increased number of AVP-IR neurons compared to control both in the PVN and in the SON ($p = 0.002$, $p < 0.001$ respectively). In the Hyper + A1254 group, the number of AVP-IR neurons was similar to that of the control group, but significantly lower compared to the Hyper groups in PVN and SON ($p = 0.026$, $p < 0.001$ respectively). The Hyper + A1254 group showed a significant decrease in the number of neurons in the SON when it was compared with its own control, the A1254 group ($p = 0.002$) (Fig. 4B).

In the case of DE-71 exposure, the one-way ANOVA showed significant differences between treatment groups in PVN ($F_{3,57} = 12.49$, $p < 0.001$) and SON ($F_{3,32} = 25.96$, $p < 0.001$) (Fig. 4C, D). Pos-hoc multiple comparisons showed that the number of AVP-IR neurons in the SON increased significantly in DE-71 group ($p < 0.001$) compared to the control. Hyper groups from PVN and SON had a significantly increased number of AVP-IR neurons compared to the control ($p = 0.003$, $p < 0.001$ respectively). When compared Hyper + DE-71 with its own control, the DE-71 group, there was a significant decrease in the number of neurons in the SON ($p < 0.001$) (Fig. 4D). The Hyper + DE-71 groups showed a significant decrease in the number of AVP-IR neurons compared to the Hyper groups in both nuclei ($p < 0.001$ both). These results were similar to those observed for the A1254 exposed group (Fig. 4B, D).

3.3.1. Cell count analysis of Nissl staining. We used alternating brain sections containing medial PVN and SON that were not processed for AVP immunohistochemistry. Normosmotic control and A1254- and DE-71-treated rats were randomly chosen from three different litters. There was no statistically significant difference in cell counts between groups in PVN ($F_{2,29} = 1.48$, $p = 0.243$) and SON ($F_{2,34} = 0.09$, $p = 0.914$). The mean values ± s.e.m. from PVN and SON were graphed (Fig. 4E, F). Further, Nissl-stained neurons seemed to have normal morphological characteristics in all groups.

3.4. cFOS mRNA expression after perinatal exposure to A1254

The cFOS mRNA expression was assessed to demonstrate if neurons of PVN and SON were activated. cFOS genes were evaluated together with the reference gene 18S ribosomal RNA. Males and females perinatally exposed to A1254 and subjected to prolonged osmotic activation were evaluated by two-way ANOVA. The IOD data indicated no statistically significant differences between sexes, for the PVN ($F_{1,15} = 2.04$, $p = 0.174$) or SON ($F_{1,16} = 3.32$, $p = 0.087$), nor did it show any interaction between sex and treatment in the PVN ($F_{3,15} = 1.18$, $p = 0.35$) or SON ($F_{3,16} = 0.26$, $p = 0.857$). As expected, there was a significant differences between treatment groups in PVN ($F_{3,15} = 15.2$, $p < 0.001$) or in SON ($F_{3,16} = 22.79$, $p < 0.001$). Post-hoc multiple comparisons indicated that Hyper groups from PVN and SON showed no significant increase of cFOS mRNA compared to control groups ($p = 0.086$, $p = 0.366$ respectively). However Hyper + A1254 group displayed the highest cFOS mRNA expression in PVN and SON with a statistically significant increase as compared to control ($p < 0.001$ both); as compared to A1254 groups (PVN $p = 0.002$; SON $p < 0.001$) and as compared to Hyper ($p = 0.002$, $p < 0.001$ respectively), (Fig. 5A, B).

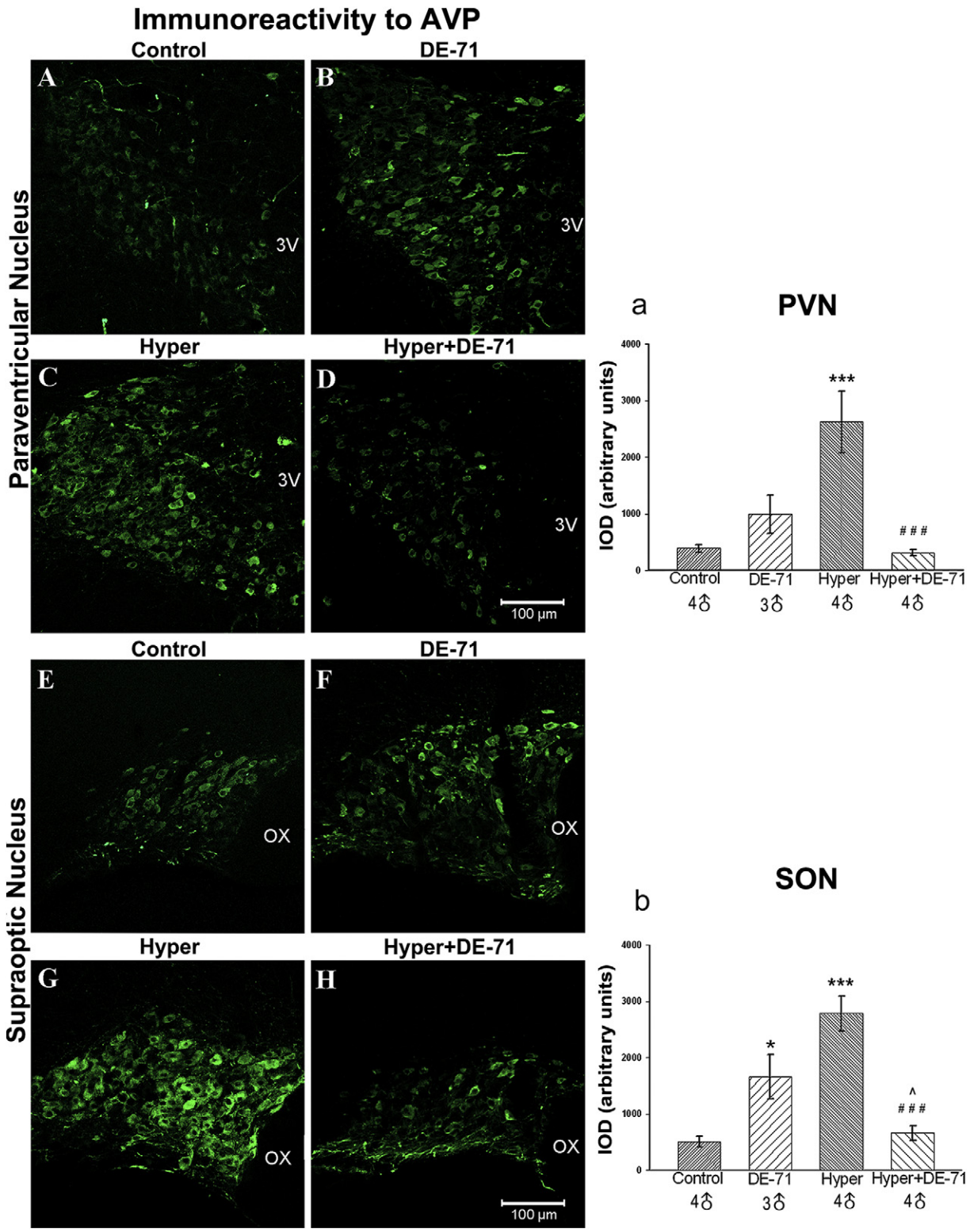

Fig. 3. Effects of perinatal exposure to DE-71 on AVP immunoreactivity (IR) in 3-month-old Wistar males rats. LEFT: Panel of representative confocal images of PVN and SON coronal sections with AVP-IR: control rats (images A and E); DE-71-treated rats (30 mg/kg/day) (B and F); hyperosmotic salt-loaded rats (Hyper) (C and G); and hyperosmotic DE-71-treated rats (Hyper + DE-71; D and H). AVP-IR increased in DE-71-treated and Hyper rats. In contrast, there was not physiological increase in staining intensity and number of AVP-IR neurons in Hyper + DE-71 rats. These results were confirmed with the IOD evaluation as showed in the graphs. RIGHT: The graphs show the effects of DE-71 on AVP-IR IOD in the PVN (a) and the SON (b). The bars represent mean values ± s.e.m. The symbols represent statistical significance as determined by one-way ANOVA and Holm-Sidak post-hoc. Asterisks (*) compared to control, number symbols (#) compared to Hyper and carets (^) compared to DE-71 treatment ($^{*,\wedge} = p < 0.05$; $^{***,\#\#\#} = p < 0.001$). Abbreviations: third ventricle (3V); optic chiasm (OX); Bar = 100 μm.

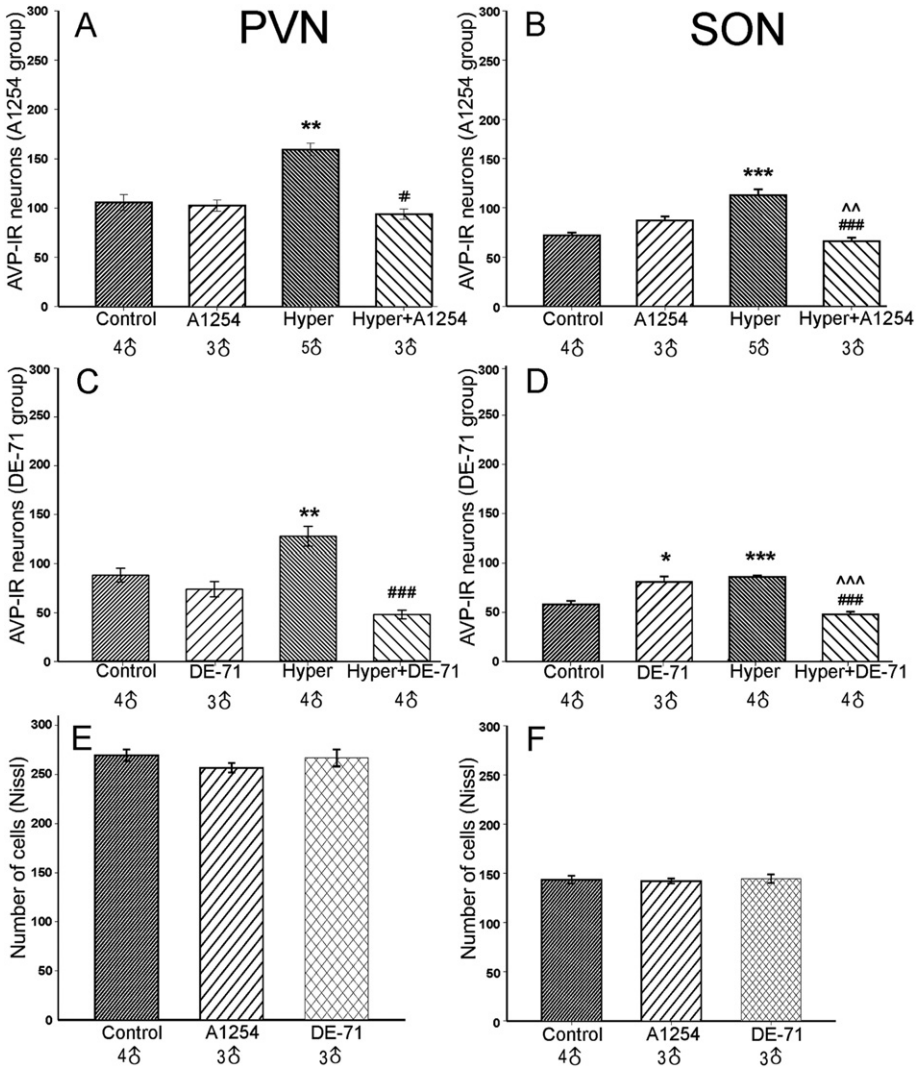

Fig. 4. Effects of perinatal exposure to A1254 or DE-71 on the number of AVP-IR neurons and Nissl-stained cells, from the PVN and SON (A, B, C, D in 3-month-old male rats during normosmotic and hyperosmotic conditions). Mean values for AVP-IR neurons increased significantly after salt loading in vehicle-treated rats (Hyper) but not in salt loaded A1254- and DE-71-treated rats (Hyper + A1254; A and B; Hyper + DE-71; C and D).These groups showed a significant decrement when compared with Hyper groups. Graphs E and F showed no change in the number of PVN and SON Nissl-stained cells of adult male rats perinatally exposed to A1254 or DE-71 (30 mg/kg). The bars represent mean ± s.e.m. values of AVP-IR neurons, and Nissl-stained cells in control, A1254- and DE-71-treated rats. The symbols represent statistical significance as determined by one-way ANOVA and Holm-Sidak post-hoc. Asterisks (*) compared to control, number symbols (#) compared to Hyper and carets (^) compared to A1254 or DE-71 treatment ($^{*,\#}p < 0.05$; **, $^{\wedge\wedge}p < 0.01$; ***, ###, $^{\wedge\wedge\wedge}p < 0.001$).

3.5. In situ hybridization histochemistry

In situ hybridization allowed us to identify and localize AVP mRNA expression within the PVN and SON. Developed silver grains of the film, denoting AVP mRNA, were widely distributed in all MNCs and some parvocellular neurons in male and female PVN and SON brain sections (Fig. 6). IOD data from males and females were evaluated with two-way ANOVA. The test indicated no statistically significant differences between sexes in the PVN ($F_{1,320} = 2.11$, $p = 0.147$) and SON ($F_{1,249} < 0.001$, $p = 0.98$). There was statistically significant differences in the mean IOD values between the treated groups (PVN; $F_{3,320} = 33.75$, $p < 0.001$, and SON; $F_{3,249} = 24.35$, $p < 0.001$). In addition, there was an interaction between sex and treatment in the PVN ($F_{3,20} = 3.46$, $p = 0.017$). Post-hoc multiple comparisons indicated a significant increase in IOD values of AVP mRNA in the Hyper groups when compared to the control in the PVN for males and females ($p < 0.001$, $p < 0.004$ respectively) and from SON in both sexes ($p < 0.001$; Fig. 6a, b). Comparison of control and A1254-exposed rats revealed no significant differences. However, A1254 treatment blunted AVP mRNA levels in animals subjected to prolonged hyperosmotic challenge, although some clusters with high signal intensity remained in the PVN and SON (Fig. 6D, H). When compared with the Hyper group, the AVP mRNA values for Hyper + A1254 decreased significantly in the PVN ($p < 0.001$ for both males and females) and SON ($p < 0.001$). The percentage decrease of Hyper + A1254 compared to the Hyper group was 68.12% in the males and 63.86% in the females in the PVN, and an average of 54.57% for both males and females in the SON. There were not differences between males and females within control, A1254 and Hyper + A1254 groups ($p > 0.05$) in the PVN, but there was a significant sex difference within the Hyper groups ($p = 0.005$).

4. Discussion

4.1. Perinatal exposure to A1254 and DE-71 disrupts AVP responses to hyperosmotic challenge in the PVN and SON of adult rats

This study demonstrates that perinatal exposure to organohalogen pollutants such as PCBs and PBDEs adversely affects the vasopressinergic system in adult rats. This effect was evident when the MNC system was stimulated by physiological demand such as

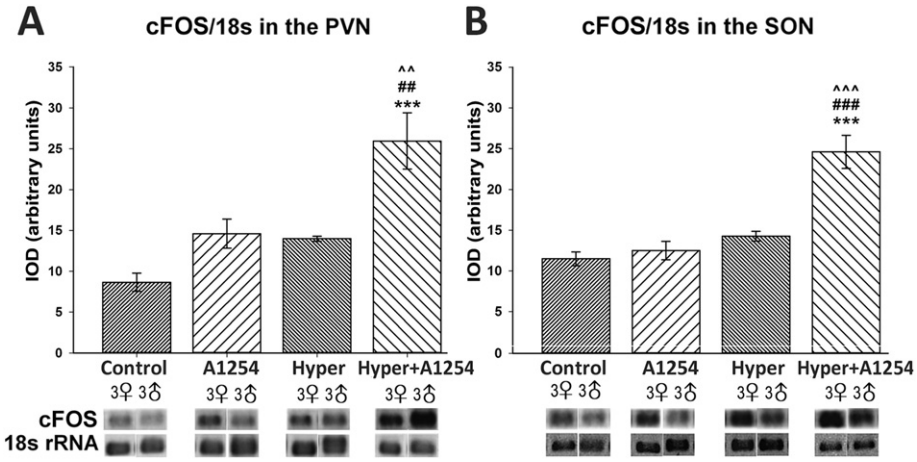

Fig. 5. Effects of perinatal exposure to A1254 on semiquantitative endpoint RT-PCR analysis of cFOS mRNA in 3-month-old males and females Wistar rats. Analyses of micropunches taken from the PVN (A) and the SON (B) were carried out in control rats (oil vehicle and normosmotic), rats perinatally exposed to A1254, rats hyperosmotically stimulated (Hyper), and rats treated with A1254 and prolonged salt-loading (Hyper + A1254). Densitometric analyses (arbitrary units) for cFOS mRNA normalized to the 18S rRNA reference gene revealed that there were no significant differences between sexes and no iteractions between sex and treatment. This is the reason that it is depicted as a single group. The A1254 and Hyper groups increased lightly but did not were significantly different compared to control group. The Hyper + A1254 groups for both PVN and the SON showed the greatest increase when compared to control, A1254 and Hyper groups. The bars represent mean IOD ± s.e.m. Below each bar there is one example from each sex of the electrophoresis bands from cFos and 18S rRNA. Statistical significance was determined by two-way ANOVA and Holm-Sidak post-hoc test. The symbols represent statistical significance, asterisks (*) compared to control, number symbols (#) compared to Hyper and carets (^) compared to A1254 or DE-71 treatment (***, ###, $^{\wedge\wedge\wedge}p < 0.001$).

after acute or chronic hyperosmotic challenges. As previously reported, hyperosmotic stimulus promotes an increase in AVP content in the hypothalamic PVN and SON and plasma AVP release. Circulating AVP leads to water retention by the kidneys and maintains plasma volume and osmolality (Ludwig et al., 1994; Weitzman and Kleeman, 1979). Also, hyperosmotic stimulation promotes release of AVP from somatodendritic components of MNCs (central AVP release) which autoregulates plasma AVP release to prevent excessive axonal AVP release during physiological demand (Liu et al., 1996; Ludwig et al., 1994). The rise in AVP content within MNC nuclei is a normal neuroendocrine response by the hypothalamo-neurohypophysial system to an increased physiological demand (Amaya et al., 1999; Bourque, 2008; Johnson and Thunhorst, 1997). This is also accomplished by increased hydration via water drinking, in the salt-loaded model and in acute hyperosmotic challenge the animals were not allowed to drink water, thereby they were forcing the system to maintain osmotic balance (Leng et al., 2001, 1999; Ludwig et al., 1996). The expected physiological increase in AVP-IR in salt-loaded rats (Hyper group) (Fig. 1C, G; Fig. 3C, G) was found in cell bodies in both the PVN and the SON, mainly in MNCs, but also in parvocellular neurons as reported by our lab and others (Amaya et al., 1999; Elgot et al., 2012; Gamrani et al., 2011; Whitnall and Gainer, 1985). The large increase in immunoreactivity to AVP-neurophysin antibody is representative of the AVP peptide and has been shown to be associated with secretory granules in MNCs (Ben-Barak et al., 1985; Whitnall and Gainer, 1985). The quantified values of IOD should not be taken as a linear index of the intracellular concentrations of the peptide, as the size of the sample was not large (3–5 rats per treatment, over six slides per nucleus -two nuclei for brain). In spite of these limitations, the observed AVP IOD values likely reflect changes in AVP content within both the PVN and the SON. Our results showed that adult rats (3 months old) perinatally exposed to commercial PCB and PBDE mixtures (A1254 and DE-71, respectively) and subjected to hyperosmotic challenge suppress the upregulation of AVP content in MNCs in the hypothalamic PVN and SON. Densitometry results suggested uniform depletion of AVP content in the neuroendocrine cells of these nuclei compared to Hyper groups (Fig. 1D, H; Fig. 3D, H), since almost all neurons in MNCs of the PVN and the SON of Hyper + A1254 and Hyper + DE-71 animals showed poor immunoreactive intensity. The reduced upregulation of AVP content may occur as a result of exaggerated axonal AVP release secondary to a decrease in central AVP release caused by perinatal exposure to A1254 and DE-71 (Coburn et al., 2007, 2005). This could lead to deplete AVP stores in the hypothalamic PVN and SON and activate the synthetic machinery in the hypothalamic MNC nuclei. These stores are needed during osmotic stress and the carrying storage capacity of the system affects osmoregulation (Amaya et al., 1999; Shoji et al., 1994). SD rats perinatally exposed to A1254 displayed similar physiology to Wistar rats. In this sense there was no surprise to find similar results even when using an acute hyperosmotic challenge (Fig. 2). This suggest a fast and more direct effect on transcription and/or translation of AVP and a permanent deficit in the neuroendocrine functions of MNCs both in Wistar and Sprague-Dawley rats.

In the control normosmotic group, AVP-IR in fibers and cell bodies showed basal staining similar to that found by other authors using the same antibody (Ben-Barak et al., 1985; Whitnall and Gainer, 1985; Whitnall et al., 1985). However, normosmotic rats exposed to either A1254 or DE-71 showed increased AVP-IR, which was statistically significant in the PVN of A1254-exposed and the SON of DE-71-exposed males (Figs. 1B, a, and 3F, b). The normosmotic rats perinatally exposed to A1254 showed a non-significant increase (7%) in the osmolality values (Table 2), a significant increase in immunoreactivity (Fig. 1Ba), and a similar trend in the number of AVP-IR neurons (Fig. 4B). Similarly, under basal normosmotic conditions, DE-71-treated male rats showed elevated AVP-IR in the SON (Fig. 3F, b; Fig. 4D) in conjunction with normal plasma osmolality (Table 2). However, normosmotic A1254-treated male rats displayed elevated plasma osmolality without showing reduced AVP-IR, a result that may be explained by negative effects of A1254 on kidney function that can impact osmoregulation (Esteban et al., 2014). In combination, these results indicate a disrupted AVP system under basal normosmotic conditions.

In the groups of exposed and subjected to the hyperosmotic challenge rats (Hyper + A1254 and Hyper + DE-71) the osmolality values were the greatest, indicating that body water balance was compromised and, hence, osmoregulation was affected (Table 2). These groups also showed the lowest AVP-IR densities indicating that their deficient osmoregulation may be due to disregulated AVP signaling (Coburn et al., 2005; Shah et al., 2011). The effects of organohalogen contamination may have significant consequences for physiological homeostasis dependent on AVP. We and others have previously shown that PCBs and PBDEs affect thyroid hormones, alter osmoregulation and cardiovascular parameters and damage kidney function (Albina et al., 2010; Brouwer et al., 1998; Kodavanti and Curras-Collazo, 2010; Li et al.,

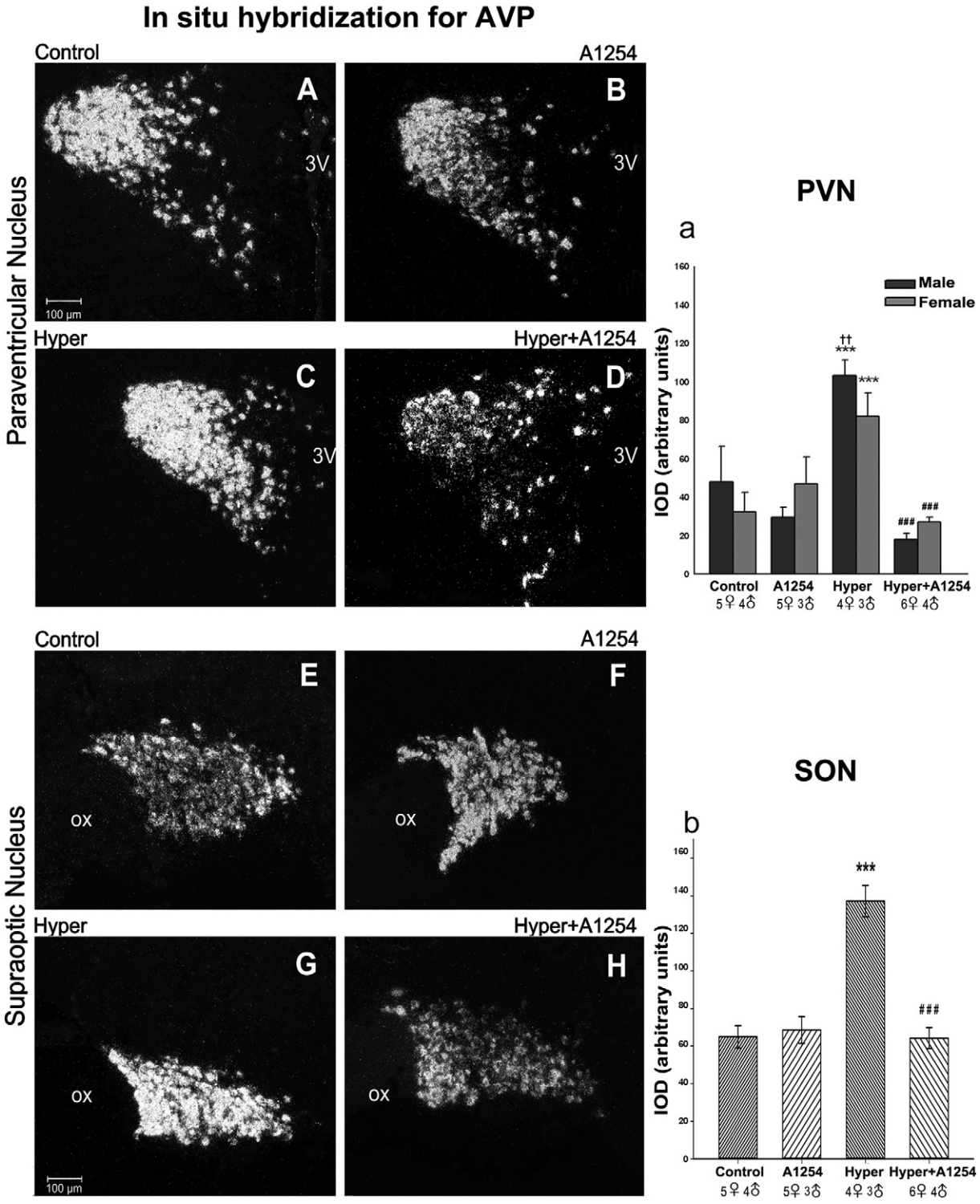

Fig. 6. Effects of perinatal exposure to A1254 on AVP mRNA expression in PVN and SON of male and female Wistar rats. mRNAs were detected using in situ hybridization with [^{35}S]-labeled probes. LEFT. Dark-field representative images from male rats of PVN and SON coronal sections show AVP mRNA in the PVN and SON in control, A1254, Hyper, and Hyper + A1254 groups. In the Hyper group, AVP mRNA increased both in the PVN and the SON as compared to control (C and G). In contrast, a decrease in the AVP mRNA of neurons occurred after hyperosmotic stimulation in the Hyper + A1254 as compared to Hyper. RIGHT: The graphs show the IOD of ISHH of AVP mRNA in the PVN (a) and the SON (b). The ANOVA from PVN indicated no statistically significant differences between sexes but there was interaction between sex and treatment groups. In the SON there were no significant differences between sexes and no interactions between sex and treatment. This is the reason that it is depicted as a single group. In the PVN and SON the comparison of control and A1254-exposed rats revealed no significant differences. However, A1254 treatment blunted AVP mRNA levels in animals subjected to prolonged hyperosmotic challenge, although some clusters with high signal intensity remained in the PVN and SON. When compared with the Hyper group, the AVP mRNA values for Hyper + A1254 decreased significantly in the PVN and SON. The bars represent mean ± s.e.m. values. Statistical significance was determined by two-way ANOVA and Holm-Sidak post-hoc test. The symbols represent statistical significance, asterisks (*) compared to control, number symbols (#) compared to Hyper, daggers (†) compared to the other sex ($^{††}p < 0.01$, ***, $^{###}p < 0.001$). Abbreviations: third ventricle (3V); optic chiasm (OX). Calibration bar = 100 μm.

2014; Shah et al., 2011). Our collaborative group has previously shown that perinatal exposure to DE-71 leads to hyperactive cardiovascular responses to osmotic stress, which may be associated with disrupted AVP-mediated processes and/or kidney function (Shah et al., 2011). Hypothyroid agents like PCBs or PBDEs may alter AVP secretion and osmoregulation indirectly by dysregulating thyroid hormone status (Kodavanti and Curras-Collazo, 2010). Ali et al. (1985) showed that in salt-loaded rats with induced hypothyroidism, antidiuresis is affected by reducing AVP-binding sites in the kidneys (Ali et al., 1987, 1985). In the PVN and SON hypothyroidism prevents osmotically-stimulated upregulation of transcripts for nitric oxide synthase (NOS), which is required for AVP functions (Ueta et al., 1995). Related to this our group has shown persistent reduction of NOS activity in the osmotically activated MNC system after similar developmental exposure to A1254 (Coburn et al., 2015; Leon-Olea et al., 2004; Mucio-Ramírez et al., 2008). Moreover, A1254 affects the expression of aquaporin 1 (AQP1) water channels (Tewari et al., 2009), which are regulated and linked to AVP V2 receptors and nitric oxide synthase (NOS) involved in water reabsorption (Klokkers et al., 2009; Swenson et al., 1997); deficiencies in the latter has been shown to impair water retention (Ma et al., 1998).

4.2. Cell count analysis of AVP-IR and Nissl-stained neurons does not indicate MNC cell death of AVP neurons by A1254

In accordance with significant reduction of mean AVP-IR IOD in hyperosmotic groups treated with organohalogens, cell counts of AVP-IR neurons showed significant decreases in the number of positive neurons compared to the Hyper group in PVN and SON ($p < 0.001$ both; Fig. 4A, B, C, D). Exposure to PCBs and PBDEs has been reported to induce a concentration-dependent loss of cell viability and apoptosis (Bradner et al., 2013; Costa et al., 2015; Johansson et al., 2006; Sanchez-Alonso et al., 2004). Therefore, to determine whether diminished upregulation of AVP-IR in Hyper + A1254 and Hyper + DE-71 was possibly linked to MNC cell death, we counted and the total number of cells in Nissl stained neurons in the medial part of PVN and the SON of all groups. A comparison of the total number of Nissl-stained cells in control and A1254-exposed rats did not show a significant difference in adult rats (Fig. 4E, F). Nor did cresyl violet staining show apparent morphological damage in the PVN and the SON. This suggests that the neurotoxic effect of A1254 on AVP-IR was not due to cell death at these ages. This does not preclude that organohalogens may produce adverse morphological changes early in development that may be reversed and undetected in adulthood. For example, our group has demonstrated neuronal shrinkage, nuclear pyknosis, and cellular death in nitrergic neurons within MNC nuclei from A1254-treated male rats at PN10 (Coburn et al., 2015; Leon-Olea et al., 2004). Cell death was likely to have occurred at early development stages or during treatment. These changes were short-lived and not observed in adult rats under basal conditions. Transient effects on the number of mature neurons, in the hippocampal dentate gyrus, have been reported after developmental exposure to decabrominated PBDEs in rats on PN20 (Saegusa et al., 2012). As expected, hyperosmotic (Hyper) groups showed a physiological increase in AVP-IR neurons in PVN magnocellular and parvocellular regions and SON (Amaya et al., 1999). Interestingly, exposure to DE-71 alone led to a significant increase in the number of AVP-IR neurons in the SON of adult male rats (Fig. 4D). In combination, these data suggest that the decrease in AVP-IR in the hyperosmotic/treated adult groups were not due to cell death but due to depletion in AVP content. More refined studies would be required to know which mechanisms are involved in these changes.

4.3. Hyperosmotic challenge and A1254 exposure activates cFOS gene in PVN and SON neurons

To explore if reduced AVP content during prolonged hyperosmotic stress in A1254-exposed rats may be due to vasopressinergic cells not receiving sufficient activation signals from osmotic stimuli, we performed end point RT-PCR for cFOS mRNA. The results showed that Hyper + A1254 group had a marked increase in cFOS mRNA in the PVN and SON of males and females (Fig. 5). Therefore, upregulated cFOS mRNA transcript levels correlated well with the rise in plasma osmolality. However, AVP-IR did not parallel the upregulation seen in cFOS mRNA levels. Although the micropunches of PVN and SON have other types of neurosecretory cells, not only vasopressinergic neurons, the results suggest that in general the osmotic challenge induced an increase in cFOS reaction that is positive in the activation of the system. Nevertheless this activation was not enough to maintain the AVP protein levels in the nuclei. This could be due to disrupted AVP synthesis which may result, in part, from reduced somatodendritic AVP (Coburn et al., 2007, 2005), that provides local autoregulatory signals (Wotjak et al., 1994). As expected, the salt-loading induced an increase in cFOS mRNA levels in the PVN and SON of male and female control groups (Fig. 5; Leng et al., 1999). This correlates with AVP immunoreactivity and plasma osmolality increase, as discussed above. Interestingly, the euhydrated rats exposed to A1254 also showed increase cFOS tendency in the PVN but not in the SON. Under these experimentally unstimulated conditions, plasma osmolality was abnormally elevated as compared to euhydrated rats (Table 2) and the upregulated c-FOS mRNA levels were consistent with elevated AVP-IR. The specific effect on PVN and the abnormal rise in plasma osmolality under "basal" conditions could suggest the involvement of altered renal signals mediated by autonomic nerves or kidney damage. Alternatively, A1254 may have a more focused effect on AVP transcription (but see below), translation or degradation that is only effective in the absence of hyperosmotic activation. For these experiments we normalized the values with the 18S rRNA gene since it was the most stable gene (Fig. 5A, B). We also probed several reference genes that were tested to normalize the results: actin, G3PDH and cyclophilin. These genes showed changes in their levels under chronic activation (data not shown), which suggested a general systemic damage due to exposure to these organohalogens.

4.4. Perinatal exposure to A1254 suppresses the physiological increase of AVP mRNA levels in the PVN and SON during chronic hyperosmotic stress

Previous studies have shown that repeated osmotic stimulation induces a compensatory increase in AVP mRNA levels and peptide production within the PVN and SON (Amaya et al., 1999; Meister et al., 1990). To explore if reduced AVP content during chronic hyperosmotic stress in A1254-exposed rats may be due to disrupted gene expression, we performed in situ hybridization histochemistry for AVP mRNA. Measurement of AVP mRNA levels (expressed as the density of developed silver grains) showed a physiologically activated increase in the PVN and the SON of salt-loaded males and females, compared to their controls (Fig. 6C, G), a finding that has been previously reported by several authors (Amaya et al., 1999; Meister et al., 1990). In contrast, in the Hyper + A1254-exposed groups, there were no expected physiological increases in AVP mRNA levels—hence, no differences from their control groups for nucleus or sex (Fig. 6D, Ha, b). Instead, there was a significant decrease in mean AVP mRNA compared to the Hyper groups, correlating with the lack of upregulated AVP-IR on this group. For the A1254-exposed normosmotic groups there were no significant differences in mean AVP mRNA IOD values as compared to the control groups, indicating a lack of induction of AVP mRNA in response to elevated cFOS and plasma osmolality seen in this group (especially males). It is unclear how the disconnection between c-FOS and AVP mRNA occurs in the A1254 groups but it may involve changes in NOS. For example, NOS isoforms such as inducible NOS may negatively regulate AVP gene expression (Oliveira-Pelegrin et al., 2010). However, A1254 may still induce the markedly elevated AVP-IR discussed above through downstream effects on neuronal NOS. For example, a recent study by our group showed that in utero exposure to A1254 alone produces abnormally elevated neuronal NOS activity in adult rats as measured by NADPH-diaphorase staining in fixed brain tissue (Coburn et al., 2015). Our lab

and others showed that neuronal NOS is required for AVP secretion (Gillard et al., 2007; Kadowaki et al., 1994).

In conclusion, both PCBs and PBDEs disrupt basal and stimulated AVP responses in MNC nuclei. Although PVN and SON in exposed groups were activated in response to the hyperosmotic stimulus (increased cFOS), neither the rapid translation of cFOS nor AVP mRNA was enough to restore AVP content in the PVN and SON, during hyperosmotic conditions. Nor was it enough to regulate plasma osmolality, as evidenced by the fact that the highest values ($p < 0.001$) were in the Hyper treated groups especially in Hyper + A1254 group (Table 2). This could lead to serious disturbances in homeostasis. A1254 treatment alone resulted in activation of c-FOS mRNA in PVN and AVP-IR without upregulation of AVP mRNA. The mechanisms underlying these effects are unclear but may be related to the effects of PCBs on NOS which can affect AVP system at transcription and secretion levels. Other mechanisms that may have intervened to decrease AVP content during chronic osmotic stress in A1254- and DE-71-exposed rats may be disrupted downstream synthetic mechanisms. A possible mechanism may have been that dioxin-like organohalogens activate the aryl hydrocarbon receptor (AhR; Denison and Nagy, 2003; Kodavanti and Curras-Collazo, 2010). After ligand binding, a heterodimer is formed which translocates into the nucleus and links to specific DNA regions. This, in turn, regulates transcription velocity of specific genes and produces genetic alterations that modify processes and functions in the cell (Denison and Nagy, 2003; Safe et al., 1985; Tilson et al., 1998), which could partially explain the unbalanced effects on AVP mRNA and content reported here.

Further research is warranted to identify the mechanisms involved in the disruption of the AVP system by organohalogens, since the AVP system is one of the main systems necessary to maintain hydromineral homeostasis that can impact osmoregulation, cardiovascular function and central AVP-regulated behavior.

5. Conclusions

Perinatal exposure to either A1254 or DE-71 affects the AVP system similarly in males and females; this effect was more evident during the hyperosmotic challenge although significant effects were detected under basal conditions. Exposure dramatically reduces hyperosmotically stimulated responses in AVP content and mRNA expression of MNCs in the PVN and the SON. These PCBs and PBDEs seem to produce similar disruption of neuroendocrine processes. The physiological outcome of the lack of response to increment AVP content in MNC during hyperosmotic stress in A1254- or DE-71-exposed rats led to a rise in plasma osmolality, an indication of disrupted water and electrolyte balance.

Vasopressin not only participates in endocrine regulation of body fluid and cardiovascular function, but also regions such as the hypothalamus, amygdala, and hippocampus are known to contain either AVP neurons or terminals and play a role in cognitive functions and regulating complex social behaviors (Shou et al., 2017; Stoop, 2012). Our findings of AVP system disruption highlight the possibility that these organohalogens may affect those other AVP brain functions (Messer, 2010; Shou et al., 2017). More refined studies would be required to assess impacts on these functions. In addition, the high body burdens of PCBs and PBDEs in children are of particular concern. Environmental organohalogens should, therefore, be considered a public health threat that must be addressed.

Conflict of interest

All authors declare no conflict of interest.

Funding

This study was supported, in part, by the INPRFM Research Support Fund (NC143290.0), Miguel Alemán Fund, (M. León-Olea) and a grant from UC-MEXUS CONACYT (M. Curras-Collazo and M. León-Olea). M. Y. Álvarez-González received a Ph.D. scholarship from CONACyT.

Acknowledgments

We are grateful to Dr. H. Gainer (NIH) for the vasopressin antibody, F. Camacho García (INPRFM) and Fidelia Romero (IBT UNAM) for the technical support and Matt Valdez (UCR) for help with osmolality statistical analysis. Dr. Heather Patisaul from NC State University, and Dr. Joyce Royland from ISTD, USEPA are acknowledged for their helpful comments on an earlier version of this manuscript. The research described in this article has been reviewed by the National Health and Environmental Effects Research Laboratory, US Environmental Protection Agency, and approved for publication. Approval does not signify that the contents necessarily reflect the views and policies of the Agency nor does mention of trade names or commercial products constitute endorsement or recommendation for use.

References

Albina, M.L., Alonso, V., Linares, V., Belles, M., Sirvent, J.J., Domingo, J.L., Sanchez, D.J., 2010. Effects of exposure to BDE-99 on oxidative status of liver and kidney in adult rats. Toxicology 271, 51–56.

Ali, M., Rougon-Rapuzzi, G., Clos, J., 1985. Response of the hypothalamo-neurohypophyseal axis (AVP system) and the kidney to salt load in young propylthiouracil-treated rats. Horm. Metab. Res. 17, 502–506.

Ali, M., Guillon, G., Balestre, M.N., Clos, J., 1987. Effects of thyroid deficiency on the vasopressin receptors in the kidney of developing and adult rats. A comparative study of hormonal binding and adenylate cyclase activation. Horm. Metab. Res. 19, 115–121.

Amaya, F., Tanaka, M., Tamada, Y., Tanaka, Y., Nilaver, G., Ibata, Y., 1999. The influence of salt loading on vasopressin gene expression in magno- and parvocellular hypothalamic neurons: an immunocytochemical and in situ hybridization analysis. Neuroscience 89, 515–523.

Andersen, M.L., Tufik, S. (Eds.), 2016. Rodent Models as Tools in Ethical Biomedical Research, first ed. Springer International Publishing, Swizerland.

Ben-Barak, Y., Russell, J.T., Whitnall, M.H., Ozato, K., Gainer, H., 1985. Neurophysin in the hypothalamo-neurohypophysial system. I. Production and characterization of monoclonal antibodies. J. Neurosci. 5, 81–97.

Birnbaum, L.S., Staskal, D.F., 2004. Brominated flame retardants: cause for concern? Environ. Health Perspect. 112, 9–17.

Bourque, C.W., 2008. Central mechanisms of osmosensation and systemic osmoregulation. Nat. Rev. Neurosci. 9, 519–531.

Bradner, J.M., Suragh, T.A., Wilson, W.W., Lazo, C.R., Stout, K.A., Kim, H.M., Wang, M.Z., Walker, D.I., Pennell, K.D., Richardson, J.R., Miller, G.W., Caudle, W.M., 2013. Exposure to the polybrominated diphenyl ether mixture DE-71 damages the nigrostriatal dopamine system: role of dopamine handling in neurotoxicity. Exp. Neurol. 241, 138–147.

Brezner, E., Terkel, J., Perry, A.S., 1984. The effect of Aroclor 1254 (PCB) on the physiology of reproduction in the female rat—I. Comp. Biochem. Physiol. C 77, 65–70.

Brouwer, A., Morse, D.C., Lans, M.C., Schuur, A.G., Murk, A.J., Klasson-Wehler, E., Bergman, A., Visser, T.J., 1998. Interactions of persistent environmental organohalogens with the thyroid hormone system: mechanisms and possible consequences for animal and human health. Toxicol. Ind. Health 14, 59–84.

Chomczynski, P., Sacchi, N., 1987. Single-step method of RNA isolation by acid guanidinium thiocyanate-phenol-chloroform extraction. Anal. Biochem. 162, 156–159.

Chung, Y.W., Nunez, A.A., Clemens, L.G., 2001. Effects of neonatal polychlorinated biphenyl exposure on female sexual behavior. Physiol. Behav. 74, 363–370.

Coburn, C.G., Gillard, E.R., Curras-Collazo, M.C., 2005. Dietary exposure to Aroclor 1254 alters central and peripheral vasopressin release in response to dehydration in the rat. Toxicol. Sci. 84, 149–156.

Coburn, C.G., Curras-Collazo, M.C., Kodavanti, P.R., 2007. Polybrominated diphenyl ethers and ortho-substituted polychlorinated biphenyls as neuroendocrine disruptors of vasopressin release: effects during physiological activation in vitro and structure-activity relationships. Toxicol. Sci. 98, 178–186.

Coburn, C.G., Curras-Collazo, M.C., Kodavanti, P.R., 2008. In vitro effects of environmentally relevant polybrominated diphenyl ether (PBDE) congeners on calcium buffering mechanisms in rat brain. Neurochem. Res. 33, 355–364.

Coburn, C.G., Watson-Siriboe, A., Hou, B., Cheetham, C., Gillard, E.R., Lin, L., Leon-Olea, M., Sanchez-Islas, E., Mucio-Ramirez, S., Curras-Collazo, M.C., 2015. Permanently compromised NADPH-diaphorase activity within the osmotically activated supraoptic nucleus after in utero but not adult exposure to Aroclor 1254. Neurotoxicology 47, 37–46.

Costa, L.G., Pellacani, C., Dao, K., Kavanagh, T.J., Roque, P.J., 2015. The brominated flame retardant BDE-47 causes oxidative stress and apoptotic cell death in vitro and in vivo in mice. Neurotoxicology 48, 68–76.

Covaci, A., Harrad, S., Abdallah, M.A., Ali, N., Law, R.J., Herzke, D., de Wit, C.A., 2011. Novel brominated flame retardants: a review of their analysis, environmental fate and behaviour. Environ. Int. 37, 532–556.

Cunningham, E.T. Jr., Sawchenko, P.E., (1991). Reflex control of magnocellular vasopressin and oxytocin secretion. Trends Neurosci. 14, 406–411.
Currás-Collazo, M.C., 2011. Nitric oxide signaling as a common target of organohalogens and other neuroendocrine disruptors. J. Toxicol. Environ. Health B Crit. Rev. 14, 495–536.
Curras-Collazo, M.C., Dao, J., 1999. Osmotic activation of the hypothalamo-neurohypophysial system reversibly downregulates the NMDA receptor subunit, NR2B, in the supraoptic nucleus of the hypothalamus. Brain Res. Mol. Brain Res. 70, 187–196.
de Wit, C.A., 2002. An overview of brominated flame retardants in the environment. Chemosphere 46, 583–624.
de Wit, C.A., Bjorklund, J.A., Thuresson, K., 2012. Tri-decabrominated diphenyl ethers and hexabromocyclododecane in indoor air and dust from Stockholm microenvironments 2: indoor sources and human exposure. Environ. Int. 39, 141–147.
Denison, M.S., Nagy, S.R., 2003. Activation of the aryl hydrocarbon receptor by structurally diverse exogenous and endogenous chemicals. Annu. Rev. Pharmacol. Toxicol. 43, 309–334.
Dunnick, J.K., Brix, A., Cunny, H., Vallant, M., Shockley, K.R., 2012. Characterization of polybrominated diphenyl ether toxicity in Wistar Han rats and use of liver microarray data for predicting disease susceptibilities. Toxicol. Pathol. 40, 93–106.
Elgot, A., El, H.O., Gamrani, H., 2012. Structural and neurochemical plasticity in both supraoptic and paraventricular nuclei of hypothalamus of a desert rodent *Meriones shawi* after a severe dehydration versus opposite treatment by rehydration: GFAP and vasopressin immunohistochemical study. Neurosci. Lett. 515, 55–60.
Esteban, J., Elabbas, L.E., Borg, D., Herlin, M., Åkesson, A., Barber, X., Hamscher, G., Nau, H., Bowers, W.J., Nakai, J.S., Viluksela, M., Håkansson, H., 2014. Gestational and lactational exposure to the polychlorinated biphenyl mixture Aroclor 1254 modulates retinoid homeostasis in rat offspring. Toxicol. Lett. 229, 41–51.
Faroon, O.M., Keith, S., Jones, D., de, R.C., 2001. Effects of polychlorinated biphenyls on development and reproduction. Toxicol. Ind. Health 17, 63–93.
Gabrielsen, G.W., Skaare, J.U., Polder, A., Bakken, V., 1995. Chlorinated hydrocarbons in glaucous gulls (*Larus hyperboreus*) in the southern part of Svalbard. Sci. Tot. Environ. **160/161**, 337–346.
Gamrani, H., Elgot, A., El, H.O., Fevre-Montange, M., 2011. Cellular plasticity in the supraoptic and paraventricular nuclei after prolonged dehydration in the desert rodent *Meriones shawi*: Vasopressin and GFAP immunohistochemical study. Brain Res. 1375, 85–92.
Gillard, E.R., Coburn, C.G., de, L.A., Snissarenko, E.P., Bauce, L.G., Pittman, Q.J., Hou, B., Curras-Collazo, M.C., 2007. Vasopressin autoreceptors and nitric oxide-dependent glutamate release are required for somatodendritic vasopressin release from rat magnocellular neuroendocrine cells responding to osmotic stimuli. Endocrinology 148, 479–489.
Hamers, T., Kamstra, J.H., Sonneveld, E., Murk, A.J., Kester, M.H., Andersson, P.L., Legler, J., Brouwer, A., 2006. In vitro profiling of the endocrine-disrupting potency of brominated flame retardants. Toxicol. Sci. 92, 157–173.
Hatton, G. I., Armstrong, W. E., Gregory, W. A., (1978). Spontaneous and osmotically-stimulated activity in slices of rat hypothalamus. Brain Res. Bull. 3, 497–508.
Jacobson, J.L., Fein, G.G., Jacobson, S.W., Schwartz, P.M., Dowler, J.K., 1984. The transfer of polychlorinated biphenyls (PCBs) and polybrominated biphenyls (PBBs) across the human placenta and into maternal milk. Am. J. Public Health 74, 378–379.
Johansson, C., Tofighi, R., Tamm, C., Goldoni, M., Mutti, A., Ceccatelli, S., 2006. Cell death mechanisms in AtT20 pituitary cells exposed to polychlorinated biphenyls (PCB 126 and PCB 153) and methylmercury. Toxicol. Lett. 167, 183–190.
Johnson, A.K., Thunhorst, R.L., 1997. The neuroendocrinology of thirst and salt appetite: visceral sensory signals and mechanisms of central integration. Front. Neuroendocrinol. 18, 292–353.
Kadowaki, K., Kishimoto, J., Leng, G., Emson, P.C., 1994. Up-regulation of nitric oxide synthase (NOS) gene expression together with NOS activity in the rat hypothalamo-hypophysial system after chronic salt loading: evidence of a neuromodulatory role of nitric oxide in arginine vasopressin and oxytocin secretion. Endocrinology 134, 1011–1017.
Khan, M., Stanley, B.G., Bozzetti, L., Chin, C., Stivers, C., Currás-Collazo, M.C., 2000. *N*-methyl-D-aspartate receptor subunit NR2B is widely expressed throughout the rat diencephalon: an immunohistochemical study. J. Comp. Neurol. 428, 428–449.
Klokkers, J., Langehanenberg, P., Kemper, B., Kosmeier, S., von Bally, G., Riethmüller, C., Wunder, F., Sindic, A., Pavenstädt, H., Schlatter, E., Edemir, B., 2009. Atrial natriuretic peptide and nitric oxide signaling antagonizes vasopressin-mediated water permeability in inner medullary collecting duct cells. Am. J. Physiol. Renal Physiol. 297, F693–F703.
Kodavanti, P.R., 2005. Neurotoxicity of persistent organic pollutants: possible mode(s) of action and further considerations. Dose-Response 3, 273–305.
Kodavanti, P.R., Coburn, C.G., Moser, V.C., MacPhail, R.C., Fenton, S.E., Stoker, T.E., Rayner, J.L., Kannan, K., Birnbaum, L.S., 2010. Developmental exposure to a commercial PBDE mixture, DE-71: neurobehavioral, hormonal, and reproductive effects. Toxicol. Sci. 116, 297–312.
Kodavanti, P.R., Curras-Collazo, M.C., 2010. Neuroendocrine actions of organohalogens: thyroid hormones, arginine vasopressin, and neuroplasticity. Front. Neuroendocrinol. 31, 479–496.
Kodavanti, P.R., Kannan, N., Yamashita, N., Derr-Yellin, E.C., Ward, T.R., Burgin, D.E., Tilson, H.A., Birnbaum, L.S., 2001. Differential effects of two lots of Aroclor 1254: congener-specific analysis and neurochemical end points. Environ. Health Perspect. 109, 1153–1161.
Kodavanti, P.R., Osorio, C., Royland, J.E., Ramabhadran, R., Alzate, O., 2011. Aroclor 1254, a developmental neurotoxicant, alters energy metabolism- and intracellular signaling-associated protein networks in rat cerebellum and hippocampus. Toxicol. Appl. Pharmacol. 256, 290–299.
Kodavanti, P.R., Tilson, H.A., 2000. Neurochemical effects of environmental chemicals: in vitro and in vivo correlations on second messenger pathways. Ann. N. Y. Acad. Sci. 919, 97–105.
Kodavanti, P.R., Ward, T.R., 2005. Differential effects of commercial polybrominated diphenyl ether and polychlorinated biphenyl mixtures on intracellular signaling in rat brain in vitro. Toxicol. Sci. 85, 952–962.
Kodavanti, P.R., Ward, T.R., Derr-Yellin, E.C., Mundy, W.R., Casey, A.C., Bush, B., Tilson, H.A., 1998. Congener-specific distribution of polychlorinated biphenyls in brain regions, blood, liver, and fat of adult rats following repeated exposure to Aroclor 1254. Toxicol. Appl. Pharmacol. 153, 199–210.
LaKind, J.S., Berlin Jr., C.M., Sjödin, A., Turner, W., Wang, R.Y., Needham, L.L., Paul, I.M., Stokes, J.L., Naiman, D.Q., Patterson Jr., D.G., 2009. Do human milk concentrations of persistent organic chemicals really decline during lactation? Chemical concentrations during lactation and milk/serum partitioning. Environ. Health Perspect. 117, 1625–1631.
Lang, V., 1992. Polychlorinated biphenyls in the environment. J. Chromatogr. 595, 1–43.
Leng, G., Brown, C.H., Bull, P.M., Brown, D., Scullion, S., Currie, J., Blackburn-Munro, R.E., Feng, J., Onaka, T., Verbalis, J.G., Russell, J.A., Ludwig, M., 2001. Responses of magnocellular neurons to osmotic stimulation involves coactivation of excitatory and inhibitory input: an experimental and theoretical analysis. J. Neurosci. 21, 6967–6977.
Leng, G., Brown, C.H., Russell, J.A., 1999. Physiological pathways regulating the activity of magnocellular neurosecretory cells. Prog. Neurobiol. 57, 625–655.
Leon-Olea, M., Martyniuk, C. J., Orlando, E. F., Ottinger, M. A., Rosenfeld, C. S., Wolstenholme, J. T., Trudeau, V. L., (2014). Current concepts in neuroendocrine disruption. Gen. Comp. Endocrinol. 203, 158–173 65.
Leon-Olea, M., Talavera-Cuevas, E., Sanchez-Islas, E., Mucio-Ramirez, S., Miller-Perez, C., Coburn, C., Gillard, E., Curras-Collazo, M., 2004. Effects of polychlorinated biphenyls on nitrergic neurons and nitric oxide synthase activity in rat pups brain. Program No. 759.10, Society for Neuroscience Abstract, 34th Annual Meeting Society For Neuroscience October 22–27, San Diego, CA.
Li, M., Liu, Z., Gu, L., Yin, R., Li, H., Zhang, X., Cao, T., Jiang, C., 2014. Toxic effects of decabromodiphenyl ether (BDE-209) on human embryonic kidney cells. Front. Genet. 5, 118.
Liu, H.W., Wang, Y.X., Crofton, J.T., Funyu, T., Share, L., 1996. Central vasopressin blockade enhances its peripheral release in response to peripheral osmotic stimulation in conscious rats. Brain Res. 719, 14–22.
Ludwig, M., Callahan, M.F., Neumann, I., Landgraf, R., Morris, M., 1994. Systemic osmotic stimulation increases vasopressin and oxytocin release within the supraoptic nucleus. J. Neuroendocrinol. 6, 369–373.
Ludwig, M., Leng, G., 1998. Intrahypothalamic vasopressin release. An inhibitor of systemic vasopressin secretion? Adv. Exp. Med. Biol. 449, 163–173.
Ludwig, M., Williams, K., Callahan, M.F., Morris, M., 1996. Salt loading abolishes osmotically stimulated vasopressin release within the supraoptic nucleus. Neurosci. Lett. 215, 1–4.
Ma, T., Yang, B., Gillespie, A., Carlson, E.J., Epstein, C.J., Verkman, A.S., 1998. Severely impaired urinary concentrating ability in transgenic mice lacking aquaporin-1 water channels. J. Biol. Chem. 273, 4296–4299.
Mariussen, E., Fonnum, F., 2006. Neurochemical targets and behavioral effects of organohalogen compounds: an update. Crit. Rev. Toxicol. 36, 253–289.
McKinney, J.D., Waller, C.L., 1994. Polychlorinated biphenyls as hormonally active structural analogues. Environ. Health Perspect. 102, 290–297.
Meister, B., Cortes, R., Villar, M.J., Schalling, M., Hokfelt, T., 1990. Peptides and transmitter enzymes in hypothalamic magnocellular neurons after administration of hyperosmotic stimuli: comparison between messenger RNA and peptide/protein levels. Cell Tissue Res. 260, 279–297.
Messer, A., 2010. Mini-review: polybrominated diphenyl ether (PBDE) flame retardants as potential autism risk factors. Physiol. Behav. 100, 245–249.
Mucio-Ramírez, S., Miller-Pérez, C., Sánchez-Islas, E., Currás-Collazo, M., León-Olea, M., 2008. Derangement of hyphothalamic nitric oxide synthase activity in osmotic stressed rats exposed to Aroclor 1254 in utero. Society for Neuroscience 38th Annual Meeting, November 15–19, abs. 780.3/QQ31, Washington, DC.
Ness, D.K., Schantz, S.L., Moshtaghian, J., Hansen, L.G., 1993. Effects of perinatal exposure to specific PCB congeners on thyroid hormone concentrations and thyroid histology in the rat. Toxicol. Lett. 68, 311–323.
Neumann, I.D., Landgraf, R., 2012. Balance of brain oxytocin and vasopressin: implications for anxiety, depression, and social behaviors. Trends Neurosci. 35, 649–659.
Palkovits, M.B.M., 1988. Maps and Guide to Microdissection of the Rat Brain. Elsevier Science, New York.
Paxinos, G., Watson, C., 1998. The Rat Brain in Stereotaxic Coordinates. 4th ed. Elsevier Academic Press, San Diego.
Oliveira-Pelegrin, G.R., de Azevedo, S.V., Yao, S.T., Murphy, D., Rocha, M.J., 2010. Central NOS inhibition differentially affects vasopressin gene expression in hypothalamic nuclei in septic rats. J Neuroimmunol. 227, 80–86.
Pittman, Q.J., Bagdan, B., 1992. Vasopressin involvement in central control of blood pressure. Prog. Brain Res. 91, 69–74.
Rickert, D.E., Dent, J.G., Cagen, S.Z., McCormack, K.M., Melrose, P., Gibson, J.E., (1978). Distribution of polybrominated biphenyls after dietary exposure in pregnant and lactating rats and their offspring. Environ. Health Perspect., **23**:63–6.
Riphagen, C.L., Pittman, Q.J., 1986. Arginine vasopressin as a central neurotransmitter. Fed. Proc. 45, 2318–2322.
Royland, J.E., Kodavanti, P.R., 2008. Gene expression profiles following exposure to a developmental neurotoxicant, Aroclor 1254: pathway analysis for possible mode(s) of action. Toxicol. Appl. Pharmacol. 231, 179–196.
Saegusa, Y., Fujimoto, H., Woo, G.H., Ohishi, T., Wang, L., Mitsumori, K., Nishikawa, A., hibutani, M., 2012. Transient aberration of neuronal development in the hippocampal dentate gyrus after developmental exposure to brominated flame retardants in rats. Arch. Toxicol. 86, 1431–1442.
Safe, S., 1993. Toxicology, structure-function relationship, and human and environmental health impacts of polychlorinated biphenyls: progress and problems. Environ. Health Perspect. 100, 259–268.

Safe, S., Bandiera, S., Sawyer, T., Robertson, L., Safe, L., Parkinson, A., Thomas, P.E., Ryan, D.E., Reik, L.M., Levin, W., Denomme, M.A., Fujita, T., 1985. PCBs: structure-function relationships and mechanism of action. Environ. Health Perspect. 60, 47–56.

Sanchez, E., Vargas, M.A., Singru, P.S., Pascual, I., Romero, F., Fekete, C., Charli, J.L., Lechan, R.M., 2009. Tanycyte pyroglutamyl peptidase II contributes to regulation of the hypothalamic-pituitary-thyroid axis through glial-axonal associations in the median eminence. Endocrinology 150, 2283–2291.

Sanchez-Alonso, J.A., Lopez-Aparicio, P., Recio, M.N., Perez-Albarsanz, M.A., 2004. Polychlorinated biphenyl mixtures (Aroclors) induce apoptosis via Bcl-2, Bax and caspase-3 proteins in neuronal cell cultures. Toxicol. Lett. 153, 311–326.

Schrier, R.W., Martin, P.Y., 1998. Recent advances in the understanding of water metabolism in heart failure. Adv. Exp. Med. Biol. 449, 415–426.

Shah, A., Coburn, C.G., Watson-Siriboe, A., Whitley, R., Shahidzadeh, A., Gillard, E.R., Nichol, R., Leon-Olea, M., Gaertner, M., Kodavanti, P.R., Curras-Collazo, M.C., 2011. Altered cardiovascular reactivity and osmoregulation during hyperosmotic stress in adult rats developmentally exposed to polybrominated diphenyl ethers (PBDEs). Toxicol. Appl. Pharmacol. 256, 103–113.

Shoji, M., Kimura, T., Kawarabayasi, Y., Ota, K., Inoue, M., Yamamoto, T., Sato, K., Ohta, M., Funyu, T., Sonoyama, T., Abe, K., 1994. Effects of acute salt loading on vasopressin mRNA level in the rat brain. Am. J. Physiol. 266, R1591–R1595.

Shou, X.J., Xu, X.J., Zeng, X.Z., Liu, Y., Yuan, H.S., Xing, Y., Jia, M.X., Wei, Q.Y., Han, S.P., Zhang, R., Han, J.S., 2017. A volumetric and functional connectivity MRI study of brain arginine-vasopressin pathways in autistic children. Neurosci. Bull. http://dx.doi.org/10.1007/s12264-017-0109-2.

Skaare, J.U., Bernhoft, A., Derocher, A., Gabrielsen, G.W., Goksøyr, A., Henriksen, E., Larsen, H.J., Lie, E., Wiig, 2000. Organochlorines in top predators at Svalbard-occurrence, levels and effects. Toxicol. Lett. **112**–113, 103–109.

Stoop, R., 2012. Neuromodulation by oxytocin and vasopressin. Neuron 76, 142–159.

Steinberg, R.M., Juenger, T.E., Gore, A.C., 2007. The effects of prenatal PCBs on adult female paced mating reproductive behaviors in rats. Horm. Behav. 51, 364–372.

Swenson, K.L., Sands, J.M., Jacobs, J.D., Sladek, C.D., 1997. Effect of aging on vasopressin and aquaporin responses to dehydration in Fischer 344-brown-Norway F1 rats. Am. J. Physiol. 273, R35–R40.

Takagi, Y., Aburada, S., Hashimoto, K., Kitaura, T., 1986. Transfer and distribution of accumulated (14C) polychlorinated biphenyls from maternal to fetal and suckling rats. Arch. Environ. Contam. Toxicol. 6, 709–715.

Tanabe, S., Nakagawa, Y., Tatsukawa, R., 1981. Absorption efficiency and biological half-life of individual chlorobiphenyls in rats treated with kanechlor products. Agric. Biol. Chem. 45, 717–726.

Tewari, N., Kalkunte, S., Murray, D.W., Sharma, S., 2009. The water channel aquaporin 1 is a novel molecular target of polychlorinated biphenyls for in utero anomalies. J. Biol. Chem. 284, 15224–15232.

Tilson, H.A., Kodavanti, P.R., Mundy, W.R., Bushnell, P.J., 1998. Neurotoxicity of environmental chemicals and their mechanism of action. Toxicol. Lett. **102**–**103**, 631–635.

Ueta, Y., Levy, A., Chowdrey, H.S., Lightman, S.L., 1995. Hypothalamic nitric oxide synthase gene expression is regulated by thyroid hormones. Endocrinology 136, 4182–4187.

U.S. Environmental Protection Agency (USEPA), 2010. An exposure assessment of polybrominated diphenyl ethers. National Center for Environmental Assessment, Washington, DC; EPA/600/R-08/086F Available from the National Technical Information Service, Springfield, VA, and online at. http://www.epa.gov/ncea.

Viberg, H., Johansson, N., Fredriksson, A., Eriksson, J., Marsh, G., Eriksson, P., (2006). Neonatal exposure to higher brominated diphenyl ethers, hepta-, octa-, or nonabromodiphenyl ether, impairs spontaneous behavior and learning and memory functions of adult mice. Toxicol. Sci. 92, 211–218.

Waye, A., Trudeau, V.L., 2011. Neuroendocrine disruption: more than hormones are upset. J. Toxicol. Environ. Health B. Crit. Rev. 14, 270–291.

Weitzman, R.E., Kleeman, C.R., 1979. The clinical physiology of water metabolism. Part I: the physiologic regulation of arginine vasopressin secretion and thirst. West. J. Med. 131, 373–400.

Westerink, R.H., 2014. Modulation of cell viability, oxidative stress, calcium homeostasis, and voltage- and ligand-gated ion channels as common mechanisms of action of (mixtures of) non-dioxin-like polychlorinated biphenyls and polybrominated diphenyl ethers. Environ. Sci. Pollut. Res. Int. 21, 6373–6383.

Whitnall, M.H., Gainer, H., 1985. Ultrastructural immunolocalization of vasopressin and neurophysin in neurosecretory cells of dehydrated rats. Brain Res. 361, 400–404.

Whitnall, M.H., Key, S., Ben-Barak, Y., Ozato, K., Gainer, H., 1985. Neurophysin in the hypothalamo-neurohypophysial system. II. Immunocytochemical studies of the ontogeny of oxytocinergic and vasopressinergic neurons. J. Neurosci. 5, 98–109.

Wiseman, S.B., Wan, Y., Chang, H., Zhang, X., Hecker, M., Jones, P.D., Giesy, J.P., 2011. Polybrominated diphenyl ethers and their hydroxylated/methoxylated analogs: environmental sources, metabolic relationships, and relative toxicities. Mar. Pollut. Bull. 63, 179–188.

Witt, D.M., 1995. Oxytocin and rodent sociosexual responses: from behavior to gene expression. Neurosci. Biobehav. Rev. 19, 315–324.

Wong, P.W., Brackney, W.R., Pessah, I.N., 1997. Ortho-substituted polychlorinated biphenyls alter microsomal calcium transport by direct interaction with ryanodine receptors of mammalian brain. J. Biol. Chem. 272, 15145–15153.

Wotjak, C.T., Ludwig, M., Landgraf, R., 1994. Vasopressin facilitates its own release within the rat supraoptic nucleus in vivo. Neuroreport 5, 1181–1184.

Wu, J., Teng, M., Gao, L., Zheng, M., 2011. Background air levels of polychlorinated biphenyls in China. Sci. Total Environ. 409, 1818–1823.